Journal of Environmental Management 363 (2024) 121343

Contents lists available at ScienceDirect

Journal of Environmental Management

journal homepage: www.elsevier.com/locate/jenvman

Research article

High-performance activation of ozone by sonocavitation for BTEX degradation in water

Kirill Fedorov [a], Lingshuai Kong [b], Chongqing Wang [c], Grzegorz Boczkaj [a,d,*]

[a] Gdansk University of Technology, Faculty of Civil and Environmental Engineering, Department of Sanitary Engineering, Gdansk, Poland
[b] Institute of Eco-Environmental Forensics, School of Environmental Science and Engineering, Shandong University, Qingdao, 266237, China
[c] School of Chemical Engineering, Zhengzhou University, Zhengzhou, 450001, China
[d] Gdansk University of Technology, EcoTech Center, 11/12 Narutowicza St., 80-233, Gdansk, Poland

ARTICLE INFO

Keywords:
Cavitation
Aromatic hydrocarbons
Environmental remediation
Wastewater treatment
Persistent organic pollutants

ABSTRACT

This work presents a novel advanced oxidation process (AOP) for degradation of emerging organic pollutants – benzene, toluene, ethylbenzene and xylenes (BTEXs) in water. A comparative study was performed for sonocavitation assisted ozonation under 40–120 kHz and 80–200 kHz dual frequency ultrasounds (DFUS). Based on the obtained results, the combination of 40–120 kHz i.e., low-frequency US (LFDUS) with O_3 exhibited excellent oxidation capacity degrading 99.37–99.69% of BTEXs in 40 min, while 86.09–91.76% of BTEX degradation was achieved after 60 min in 80–200 kHz i.e., high-frequency US (HFDUS) combined with O_3. The synergistic indexes determined using degradation rate constants were found as 7.86 and 2.9 for LFDUS/O_3 and HFDUS/O_3 processes, respectively. The higher extend of BTEX degradation in both processes was observed at pH 6.5 and 10. Among the reactive oxygen species (ROSs), hydroxyl radicals ($HO^{\bullet}$) were found predominant according to scavenging tests, singlet oxygen also importantly contributed in degradation, while $O_2^{\bullet-}$ radicals had a minor contribution. Sulfate (SO_4^{2-}) ions demonstrated higher inhibitory effect compared to chloride (Cl^-) and carbonate (CO_3^{2-}) ions in both processes. Degradation pathways of BTEX was proposed based on the intermediates identified using GC-MS technique.

1. Introduction

Rapid urbanization and industrialization in the absence of proper environmental management are a one of main sources of the growing emission of volatile organic compounds (VOCs) in the environment. VOCs of anthropogenic nature are considered as the contributor of air pollution indirectly causing stratospheric ozone depletion, tropospheric ozone formation, ground level smog formation as well as climate change (Zhong et al., 2017; Khan and Ghoshal, 2000). Particularly, petroleum refineries, chemical industries, textile manufacturers, paper production and food processing can be classified as the major contributors of air pollution. VOCs represent the large family of carbon-based compounds and depending on the source of emission, they can be halogenated hydrocarbons, alcohols, aldehydes, aromatics, alkenes, ketones, esters, polycyclic hydrocarbons (Kamal et al., 2016; Hashemi et al., 2020; Boczkaj et al., 2016a, 2016b, 2017). These compounds are highly toxic to human and may cause many symptoms and diseases, such as throat, eye and nose irritation, nasopharyngeal cancer, pulmonary damage, leukemia (Guo et al., 2004; Hazrati et al., 2016). As VOCs threaten the environment and public health, they attracted the global attention and strictly regulated in many countries.

As a natural constituent of a crude oil, gasoline and other petroleum-based products, BTEX enter aquatic environment due to inadequate sewage treatment practices and pipeline leakages (Emmanuel et al., 2023; Vellingiri et al., 2022). Besides, petroleum industry, the origin of BTEX contamination may include a variety of production sites, in which BTEX are utilized, such as synthesis of plastic, rubber, paintings and agriculture (Emmanuel et al., 2023; Wang et al., 1995). The maximum permissible concentration of benzene, toluene, ethylbenzene and xylenes in drinking water were estimated as 5, 1000, 700 and 1000 μg L^{-1}, respectively, according to the US Environmental Protection Agency (EPA) (Vellingiri et al., 2022; Carneiro et al., 2014). Introduced into the human body by skin contact, digestive system and inhalation, BTEX are associated with the development of various environmental diseases

* Corresponding author. Gdansk University of Technology, Faculty of Civil and Environmental Engineering, Department of Sanitary Engineering, 80 – 233 Gdansk, G. Narutowicza St. 11/12, Poland.
E-mail address: grzegorz.boczkaj@pg.edu.pl (G. Boczkaj).

https://doi.org/10.1016/j.jenvman.2024.121343
Received 27 February 2024; Received in revised form 10 May 2024; Accepted 30 May 2024

(Durmusoglu et al., 2010). Thus, low-concentration exposure to benzene is reported to induce confusion, tiredness, nausea as well as development of aplastic anemia, leukemia and solid tumors (Al-Harbi, 2019). Ethylbenzene increased the incidences of serious problems with respiratory system and kidneys. Furthermore, the environmental exposure to toluene and xylenes led to toxic effects on the nervous system, liver and kidneys (Hazrati et al., 2016). Considering the persistence of BTEX to the conventional water treatment technologies, its widespread occurrence and inherent toxicity, the development of efficient and economically viable degradation method is highly desired.

In the past few decades, advanced oxidation processes (AOPs) have been proven to satisfactory remove a wide list of persistent water pollutants (Li et al., 2024; Liu et al., 2023). AOPs consist of a set of processes which principal operation mechanism is the generation of highly oxidizing radicals. Hydroxyl ($HO^{\bullet}$) radicals with oxidation potential of 1.7–2.8 V_{NHE} are the primary species in many AOPs (e.g., Fenton's process, ozonation at pH > 7, peroxone, photocatalysis) and react with majority of organic pollutants at a rate constant of 10^6-10^9 M^{-1} s^{-1}. The rapid oxidation induced by $HO^{\bullet}$ radicals is non-selective and sufficient to attain a complete mineralization of persistent organic pollutants to CO_2 and H_2O. Among the AOPs that are utilizing $HO^{\bullet}$ radicals, ultrasound (US) emerged as promising method that can be easily applied in water and sewage treatment of larger operating scales. The formation of $HO^{\bullet}$ radicals under the action of US in liquid is associated with the term of "cold boiling" or cavitation. The cavitation can be defined as the process of formation, growth and subsequent collapse of cavitation bubbles in an extremely short interval of time (Cako et al., 2020; Fedorov et al., 2020). The collapse of cavitation bubbles releases a large magnitude of energy creating high local temperature and pressure above 5000 K and 1000 atm. Such local "hot spots" promote a variety of reactions in liquid which result in generation of $HO^{\bullet}$, $HO_2^{\bullet}$, $H^{\bullet}$ radicals and H_2O_2 (Makino et al., 1982; Adewuyi, 2001; Fitzgerald et al., 2004). Consequently, US-based treatment methods were shown sufficient to degrade *p*-nitrophenol (Pradhan and Gogate, 2010; Sivakumar et al., 2002), dyes (Cako et al., 2020; Sivakumar and Pandit, 2001), polycyclic aromatic hydrocarbons (Psillakis et al., 2004), phenol (Okouchi et al., 1992; Gogate et al., 2003a; Gągol et al., 2020), sulfide ions and organic sulfides (Gągol et al., 2019). The oxidative degradation of pollutants in water by US is attributed to the generation of highly reactive species and facilitated mass transfer in the system by liquid circulation currents and intensive turbulence (Ammar, 2016; Gągol et al., 2018a). Whereas, the utilization of sole US has been reported to rapidly transform organic substrates into short-chain organic acids or CO_2 and H_2O, it has often been challenging to achieve complete mineralization of persistent organic contaminants. The persistent pollutants can be mineralized or degraded in higher extend by integration of US with other AOPs (Gągol et al., 2018b; Zhou et al., 2008; Sun et al., 2007). The coupled processes exhibit higher degradation efficiency at lower cost compared due to the synergistic effect ensuring a greater efficacy than the cumulative effect of individual processes (Zanias et al., 2020; Nikolaou et al., 2020). Thus, US-assisted ozonation degraded 99.2% of the reactive red X–3B dye in 6 min at the initial concentration of 100 mg L^{-1} (Shen et al., 2017). Compared to sole US and O_3 processes, US/O_3 system exhibited significantly higher decolorization efficacy with the synergetic factor of 1.42. It was concluded that in the system of conjugated ozonation and sonolysis, acoustic cavitation induced played a crucial role facilitating the mass transfer of O_3 in aqueous phase. The synergistic index of 1.5 was obtained for the degradation triazophos using the combination of O_3 and US (Jawale and Gogate, 2018). Particularly, 52.4% of triazophos with the initial concentration of 20 ppm were degraded in 90 min with O_3, whereas sole US degraded 43% of triazophos. The higher extend of triazophos degradation by the hybrid technique was attributed to the increased mass transfer giving better utilization of O_3 and the enhanced amount of generated $HO^{\bullet}$ radicals. Similarly, enhanced generation of reactive radical species, such as $HO^{\bullet}$ radicals and nascent oxygen was observed in US/O_3 system during the treatment of the pharmaceutical industry effluent (Chandak et al., 2020). In this case, the COD reduction above 30% was attained after 120 min. To conclude, the synergistic effect in US/O_3 processes is attributed to acoustic cavitation, which is responsible for the effective decomposition of O_3 to yield reactive radical species. Additionally, microcirculations and turbulence in the bulk liquid induced by US waves provide an effective dispersion of O_3 thereby reducing the mass transfer resistance. Nevertheless, the sonochemical transformations (e.g., generation of $HO^{\bullet}$ radicals) in single-frequency US are limited due to non-uniform volumetric energy dissipation in the treated liquid due to directional sensitivity of the US field (Moholkar, 2009). The utilization of dual or multiple frequency US was explored to overcome the disadvantage associated with the directional sensitivity through the production of strong interference pattern in the reactor. The effect of dual-frequency US was studied in a diverse range of applications, such as sonoluminescence (Lu et al., 2003; Lee and Oh, 2011; Ciuti et al., 2000), KI oxidation (Ebrahiminia et al., 2016; Feng et al., 2002), leaching of valuable metals (Swamy and Narayana, 2001) and degradation of water pollutants (Sivakumar et al., 2002; Hua et al., 1995; Gogate et al., 2003b; Wang et al., 2006; Zhao et al., 2010).

Among AOPs combined with dual-frequency US, ozonation under dual-frequency US has been demonstrated as an effective method for water treatment application. Thus, the combination of 20 kHz–40 kHz dual-frequency US with O_3 was shown to degrade 83.8% of nitrobenzene in 60 min representing an increment of 30.6% compared the cumulative effect of sole US and O_3 (Zhao et al., 2010). Up till now, the range of selected dual frequencies applied in US/O_3 was narrow (i.e., 20 kHz–28 kHz and 20 kHz–40 kHz). Moreover, the effect on dual-frequency US on BTEX ozonation has not been reported. Herein, we extend the investigation on sonochemical transformations of O_3 occurring over acoustic cavitation induced by dual-frequency US, comparing the effect 40 kHz–120 kHz and 80 kHz–200 kHz DFUS on BTEX degradation. The outcomes of this study contribute to a more comprehensive understanding of the role of acoustic cavitation in AOPs, allowing for the optimization of operating parameters in order to achieve the highest sonochemical efficiency in US-assisted AOPs. The study concerns the radical mediated process potentially employed in water treatment industry, therefore, several operating aspects critical in practical application, such as pH, the effect of radical scavengers and co-existing anions were studied. The mechanism of BTEX degradation was proposed based on the intermediates identified by gas chromatography coupled with mass spectrometry (GC-MS). The obtained results were discussed in order to elucidate the role of combined frequencies in synergistic mechanism of US/O_3 for the degradation of BTEX in water.

2. Materials and methods

2.1. Materials

Benzene (99.7%), toluene (pure), were purchased from Chempur (Poland) and POCH (Poland), respectively. Ethylbenzene (99%) and *o*-xylene (≥98%) were purchased from Merck KGaA (Germany) and Merck Schuhard OHG (Germany), respectively. Sulfuric acid (pure, ≥98%) and sodium hydroxide (pure, ≥85%) were supplied from POCH (Poland). Potassium iodide (pure, p. a.) and sodium thiosulfate pentahydrate (acs pure p. a.) were purchased from POCH (Poland). Methanol (pure, 95%) used for quenching experiments was obtained from POCH (Poland). Sodium azide (pure p. a., 99.0%) was purchased from Chempur (Poland), while 1,4-benzoquinone (99%) was obtained from Acros Organics (Belgium). Sodium chloride (pure) was purchased from POCH (Poland), sodium carbonate (99.8%) and sodium sulfate (99.0%) were supplied from Chempur (Poland). All solutions were prepared using ultrapure quality water (18.2 MΩcm^{-1}) from Millipore® system (Direct-Q UV-R model). All chemical and solvents were used as received.

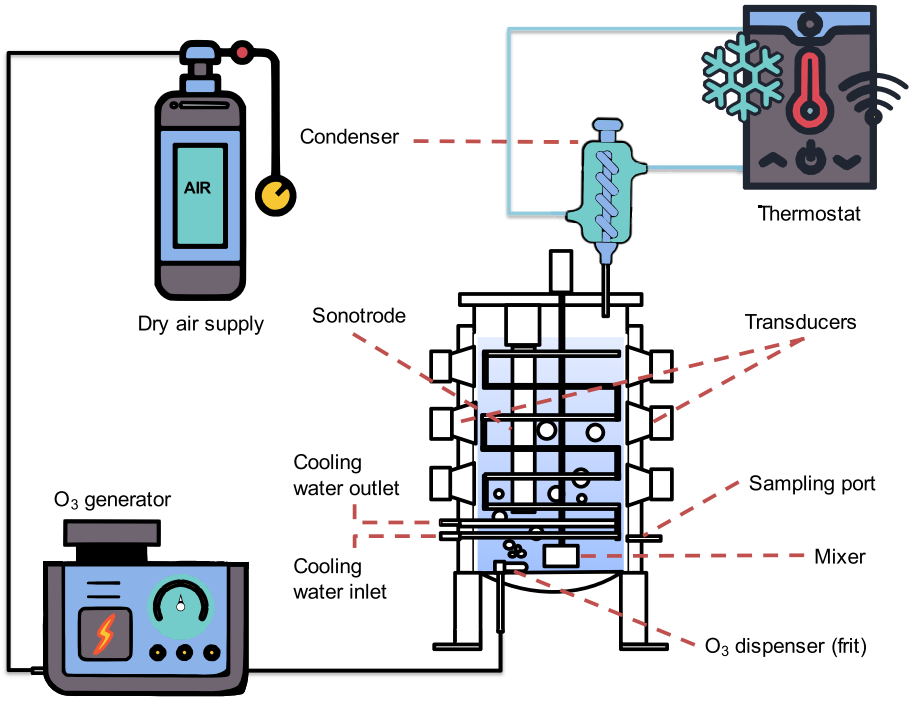

Fig. 1. Scheme of the experimental setup for BTEX ozonation under dual-frequency US.

Table 1
Pseudo-first-order kinetic model constant rates of BTEX degradation in LFDUS and HFDUS systems.

Process	Frequency	Benzene	Toluene	Ethylbenzene	*o*-Xylene
	kHz	k, min^{-1}	k, min^{-1}	k, min^{-1}	k, min^{-1}
US	40	0.0026	0.0025	0.0024	0.0021
	80	0.0039	0.0037	0.0034	0.0034
	120	0.0034	0.0030	0.0028	0.0027
	200	0.0027	0.0027	0.0030	0.0025
LFDUS	40–120	0.0064	0.0062	0.0059	0.0058
HFDUS	80–200	0.0060	0.0059	0.0061	0.0058

2.2. Experimental procedure

Ozonation experiment were performed in a custom-designed sono-reactor manufactured by Beijing Yongda Ultrasonic CO., LTD (China). The experimental setup is presented in Fig. 1. The reactor was equipped with a sonotrode, transducers, temperature sensor, mixer and cooling system. The transducers mounted on the walls of the reactor were capable to produce ultrasonic waves with a frequency of 120 kHz and 200 kHz, respectively. A sonotrode attached on the removable cover of the reactor had an operating frequency of 120 kHz and 200 kHz, respectively. A combination of 40 kHz sonotrode and 120 kHz transducers were utilized for low-frequency sonication experiments, while 80 kHz sonotrode and 200 kHz transducers – for high-frequency sonication mode. In a typical experiment, 3.8 L of model solution containing 50 ppm of BTEX (i.e. 50 mg/kg of each compound (benzene, toluene,

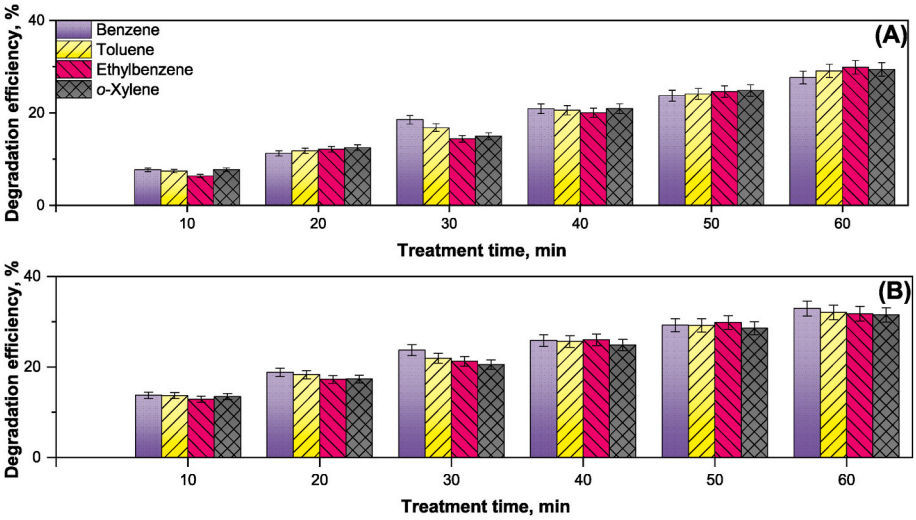

Fig. 2. Degradation efficiency of BTEX in (a) LFDUS, (b) HFDUS; $[BTEX]_0$: 50 ppm (v/v), pH 6.5, T = 20 ± 2.5 °C, US power input 600 W, US frequencies: 40/120 kHz and 80/200 kHz for LFDUS and HFDUS, respectively.

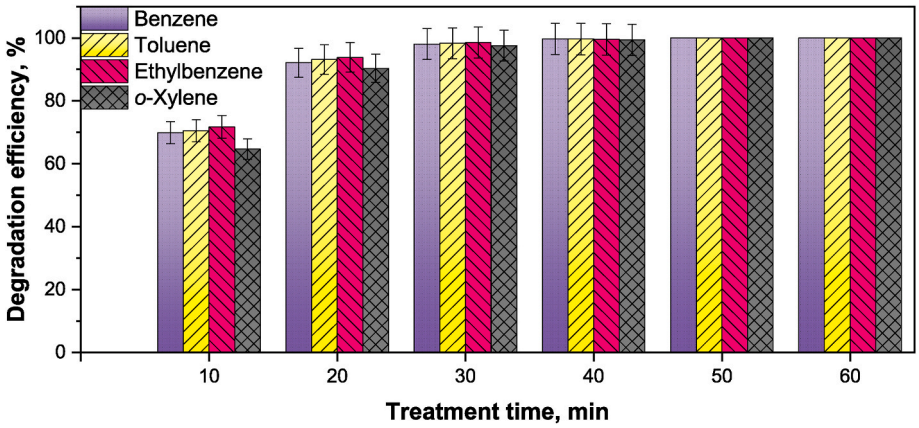

Fig. 3. Degradation efficiency of BTEX in LFDUS/O_3; $[BTEX]_0$: 50 ppm (v/v), pH 6.5, T = 20 ± 2.5 °C, O_3 flow rate 0.5 L min^{-1}, US power input 600 W, US frequencies: 40/120 kHz.

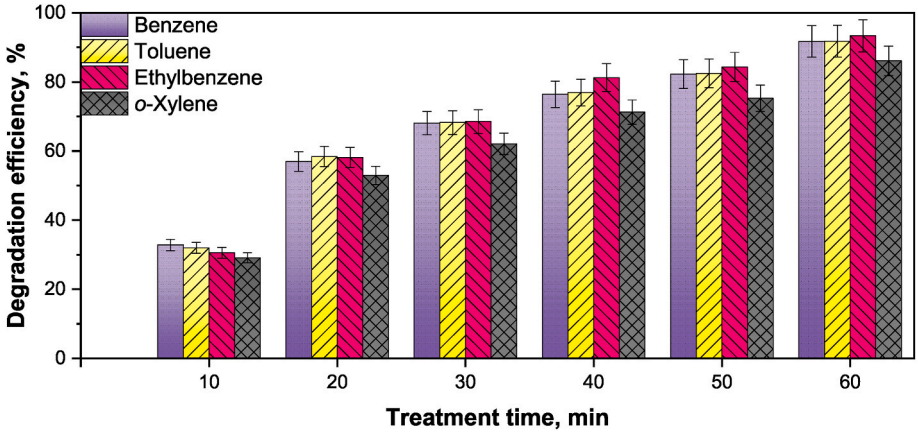

Fig. 4. Degradation efficiency of BTEX in HFDUS/O_3; $[BTEX]_0$: 50 ppm (v/v), pH 6.5, T = 20 ± 2.5 °C, O_3 flow rate 0.5 L min^{-1}, US power input 600 W, US frequencies: 80/200 kHz.

Table 2
Pseudo-first-order kinetic model constant rates of BTEX degradation in O_3-assisted processes.

Process	Frequency	Benzene	Toluene	Ethylbenzene	*o*-Xylene
	kHz	*k*, min^{-1}	*k*, min^{-1}	*k*, min^{-1}	*k*, min^{-1}
Sole O_3	–	0.0055	0.0067	0.0081	0.0067
US/O_3	40	0.0094	0.0093	0.0089	0.0070
	80	0.0144	0.0144	0.0151	0.0119
	120	0.0143	0.0152	0.0172	0.0131
	200	0.0179	0.0182	0.0200	0.0141
LFDUS/O_3	40/120	0.1431	0.1419	0.1387	0.1282
HFDUS/O_3	80/200	0.0384	0.0385	0.0425	0.0304

ethylbenzene and *o*-xylene respectively), was placed in sono-reactor and treated for 60 min at 20 ± 2 °C. A Tytan 32 ozone generator (Erem) was used for ozonation and was connected to sono-reactor by PTFE tubes. Ozone was fed using dry air as a carrier gas at a flowrate of 0.5 L min^{-1} through a porous frit at the bottom of sono-reactor to provide better distribution. Tap water was flowed continuously through stainless steel cooling coil placed in the reaction chamber to maintain constant temperature. A glass condenser was connected to ozone outlet to prevent BTEX evaporation. The condenser was connected to refrigerated circulator bath HAAKE DC30 K^{20} (Thermo Scientific, Germany) filled with methanol to maintain −5 °C. Aliquots of samples (20 mL) were collected at certain time interval for analysis. All the experiments were performed in duplicate.

2.3. Analytical methods

Sample preparation for GC-FID analysis was conducted by dispersive liquid-liquid microextraction (DLLME) using dichloromethane (POCH, Poland) as an extraction solvent and acetone (POCH, Poland) as dispersive agent. The molar ratio between dichloromethane and acetone was taken as 50:40, respectively. The quantitative analysis of BTEX content was proceeded based on the internal standard method using 4-chlorophenol (POCH, Poland) as internal standard. The detailed description of DLLME procedure is provided in previously reported studies (Makoś et al., 2018). A Clarus 500 (PerkinElmer, USA) gas chromatograph equipped with flame ionization detector (GC-FID) was used for quantitative analysis of BTEX. A capillary column (60 m × 0.32 mm ID, 1.8 μm DB624, Agilent, USA) was used for separation of analytes. Operating conditions of GC-FID were as follows: oven temperature 50 °C (5 min) ramped at 10 °C min^{-1} to 275 °C (20 min), 2 μL of the extract was injected to the GC-FID from each sample twice. The temperature of injection port and detector were 300 °C and 275 °C, respectively. The hydrogen and air flow were supplied in flow rates of 40 and 430 mL min^{-1}, respectively.

The intermediates of BTEX degradation were identified by GCMSQP2010SE (Shimadzu, Japan) gas chromatograph coupled to a mass spectrometer (GC-MS). The separation of analytes was conducted using a capillary column (100 m × 0.2 mm ID, 0.1 μm DHA, Restek, USA). The GC column operated in a temperature programmed mode with initial temperature of 40 °C (isothermal for 5 min) which ramped at 5 °C min^{-1} to 220 °C. A PGX500 hydrogen generator (PerkinElmer,

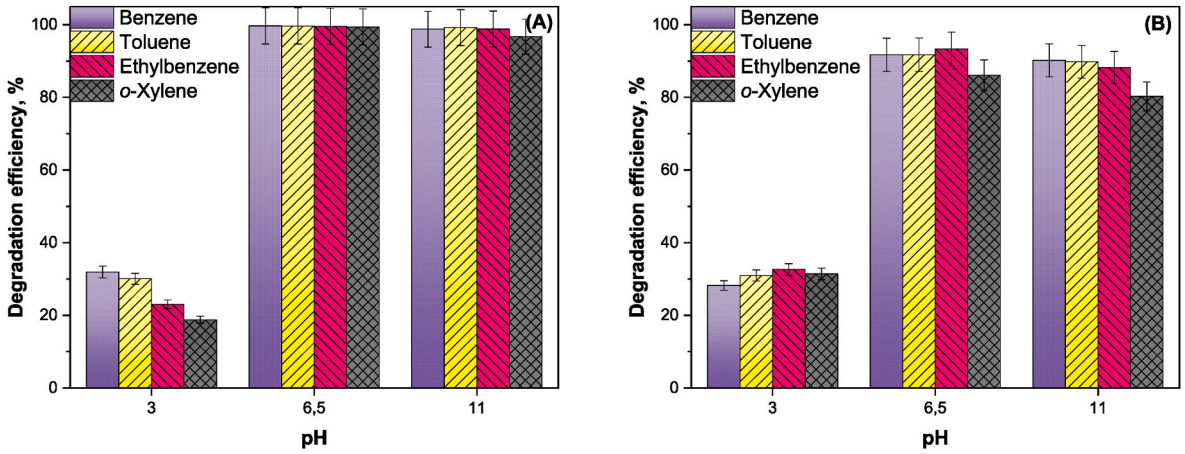

Fig. 5. Effect of pH on BTEX degradation in (a) LFDUS/O_3 and (b) HFDUS/O_3 [BTEX]$_0$: 50 ppm (v/v), pH 6.5, T = 20 ± 2.5 °C, Treatment time: 40 min for LFDUS/O_3 and 60 min for HFDUS/O_3, O_3 flow rate 0.5 L min^{-1}, US: 600 W, 40/120 kHz (LFDUS) and 80/200 kHz (HFDUS).

Table 3
Pseudo-first-order kinetic model parameters of BTEX degradation in LFDUS/O_3 and HFDUS/O_3 at various pH.

pH	Process	Benzene	Toluene	Ethylbenzene	*o*-Xylene
		k, min^{-1}	k, min^{-1}	k, min^{-1}	k, min^{-1}
3	LFDUS/O_3	0.0092	0.0091	0.0080	0.0063
	HFDUS/O_3	0.0059	0.0062	0.0062	0.0057
6.5	LFDUS/O_3	0.1431	0.1419	0.1387	0.1282
	HFDUS/O_3	0.0384	0.0385	0.0425	0.0304
11	LFDUS/O_3	0.1123	0.1233	0.1190	0.0877
	HFDUS/O_3	0.0398	0.0393	0.0371	0.0274

USA) was used to supply hydrogen at a flow rate of 1 mL min^{-1}, the temperature in GC-MS transfer line and injection port were set at 310 °C and 300 °C, respectively. A mass spectra were recorded in the range of 34–220 m/z using an electron impact ionization mode (EI 70 eV). The ionization source temperature was set at 200 °C.

The concentration of gaseous O_3 in dry air stream was determined by iodometric titration method. For this, the feed of O_3 was bubbled through two connected gas washing bottles filled with 500 mL of 2% KI (w/w). The solutions were acidified to pH 3 by adding 2 N H_2SO_4 and the compresses air stream containing O_3 was sparged through KI solution using sintered glass disc located in the bottom half of bottles. A standardized 0.01 mol L^{-1} $Na_2S_2O_3$ solution was used as a titrant in presence of 5% (w/v) starch indicator. The dose of applied O_3 was determined as 2.1 g h^{-1} and the molar ratio of BTEX to O_3 (r_{ox}) was 6.25.

3. Results and discussion

3.1. Degradation of BTEX by single and dual frequency US

Prior to evaluating the effect of dual-frequency US (DFUS), the effect of single US of different frequency on BTEX degradation was investigated. As shown in Fig. S1 (Supplementary data), 19.87, 18.04, 15.48 and 15.82% of benzene, toluene, ethylbenzene and *o*-xylene were degraded in 60 min by 80 kHz US. The rate constants of BTEX degradation observed in US-80 kHz were the highest among the studied frequencies as presented in Table 1. Next, the effect of dual frequencies was studied. As illustrated in Fig. 2a, the combination of 40 and 120 kHz (LFDUS) increased the degradation efficiency of BTEX to 28.6–32.0% after 60 min of treatment. Likewise, the combination of 80 kHz sonotrode and 200 kHz transducers (HFDUS) degraded 31.5–32.9% of BTEXs in 60 min as shown in Fig. 2b. The degradation extent of BTEXs in both cases was similar and the highest degradation was observed for benzene, while *o*-xylene was the least degraded. This observation probably indicates that the non-selective radical-induced oxidation at gas-liquid phase and bulk liquid were the main degradation sites as benzene, toluene and ethylbenzene with lower logK_{ow} were degraded in higher extend. As a part of sonochemical processes taking place in the liquid, the oxidative degradation of pollutants relates to acoustic cavitation induced by US irradiation. The localized extreme conditions created due to the adiabatic collapse of cavitation bubbles are sufficient to promote a thermal decomposition of pollutants and water. The disassociation of water occurs in both gaseous and gas-liquid phases yielding $HO^\bullet$ and $H^\bullet$ radicals along with secondary $HO_2^\bullet$ radicals in air-saturated liquids (**Eqs. 1, 2**). In the absence of scavengers, these radicals undergo recombination with formation of H_2O_2, H_2 and H_2O as shown in **Eqs. (3)–(6)** (Yusof et al., 2016; Beckett and Hua, 2000). Although, $HO^\bullet$ radicals and H_2O_2 are powerful oxidants, the degradation efficiency of BTEX in the studied single-frequency US is low due to the limited generation of ROSs.

$$H_2O \xrightarrow{\text{cavitation}} HO^\bullet + H^\bullet \quad \text{Eq. 1}$$

$$H^\bullet + O_2 \rightarrow HO_2^\bullet \quad \text{Eq. 2}$$

$$HO^\bullet + HO^\bullet \rightarrow H_2O_2 \quad \text{Eq. 3}$$

$$H^\bullet + H^\bullet \rightarrow H_2 \quad \text{Eq. 4}$$

$$HO^\bullet + H^\bullet \rightarrow H_2O \quad \text{Eq. 5}$$

$$HO_2^\bullet + HO_2^\bullet \rightarrow H_2O_2 + O_2 \quad \text{Eq. 6}$$

The synergistic index values (ξ) determined according to **Eq. (7)** were found as 1.13 and 0.94 for LFDUS and HFDUS, respectively. The synergistic effect observed in LFDUS implies that the application of DFUS increases the sonochemical yield of ROSs by acoustic cavitation and consistent with previously reported statements. In particular, it has been suggested that the cavitation bubbles affected by DFUS possess high collapse pressure and grow to the maximum size faster (Tatake and Pandit, 2002; Manickam et al., 2014). Therefore, it can be suggested that the higher collapse pressure achieved in LFDUS promoted the pyrolytic decomposition of BTEX, while the short collapse time intensified the yield of $HO^\bullet$ radicals.

$$\xi = \frac{k_{a+b}}{k_a + k_b} \quad \text{Eq. 7}$$

where k_{a+b} is the rate constant of the combined process, while k_a and k_b – rate constants of sole processes.

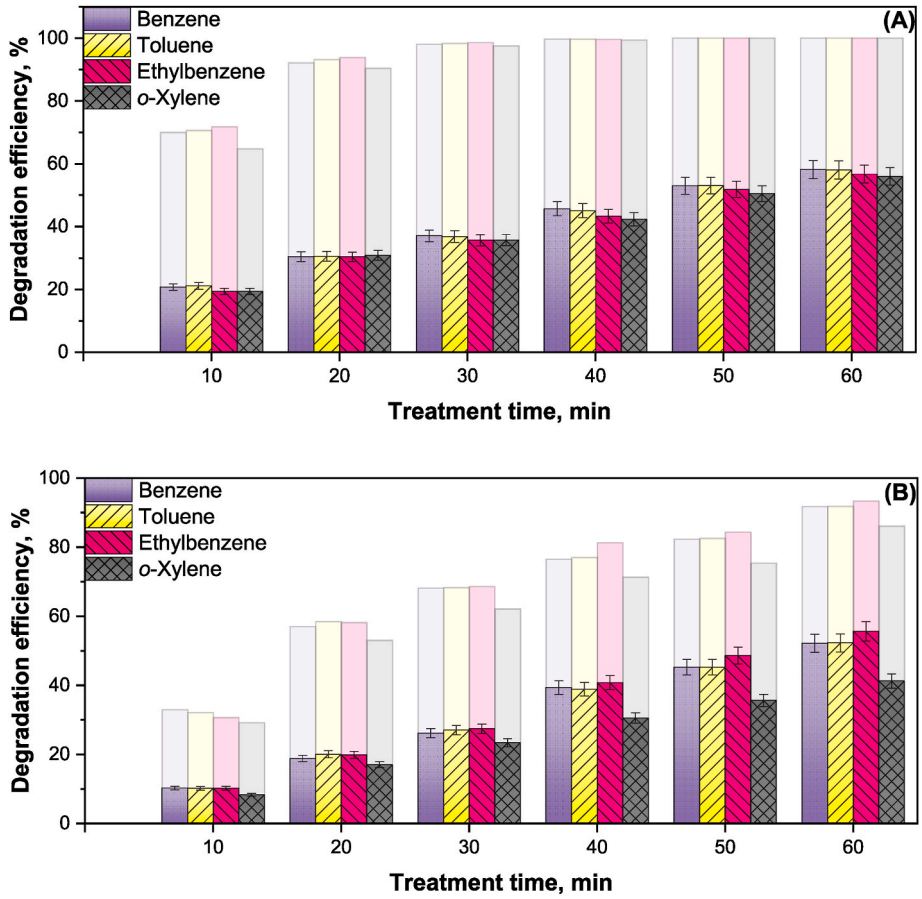

Fig. 6. Effect of MeOH on BTEX degradation in (a) LFDUS/O_3 and (b) HFDUS/O_3; $[BTEX]_0$: 50 ppm (v/v), $[O_3]$: [MeOH] = 1:10, pH 6.5, T = 20 ± 2.5 °C, O_3 flow rate 0.5 L min^{-1}, US: 600 W, 40/120 kHz (LFDUS) and 80/200 kHz (HFDUS). Shadowed data - corresponding processes without additives.

Table 4
Pseudo-first-order kinetic model parameters of BTEX degradation in LFDUS/O_3 and HFDUS/O_3 in the presence of scavengers.

Scavenger	Process	Benzene	Toluene	Ethylbenzene	*o*-Xylene
		k, min^{-1}	*k*, min^{-1}	*k*, min^{-1}	*k*, min^{-1}
MeOH	LFDUS/O_3	0.0139	0.0138	0.0134	0.0129
	HFDUS/O_3	0.0125	0.0124	0.0138	0.0089
p-BQ	LFDUS/O_3	0.0165	0.0181	0.0201	0.0166
	HFDUS/O_3	0.0210	0.0216	0.0237	0.0175
NaN_3	LFDUS/O_3	0.0052	0.0054	0.0056	0.0040
	HFDUS/O_3	0.0056	0.0056	0.0055	0.0055

3.2. Dual-frequency US combined with ozone

The hybrid process of US/O_3 is a technically simple and efficient AOP capable to ensure a rapid degradation of recalcitrant pollutants due to the synergistic effect between the coupled techniques. In order to assess the effectiveness of single-frequency US/O_3, the effect of sole ozonation and US at different frequencies coupled with O_3 were conducted and evaluated towards the degradation of BTEXs. Fig. 2S depicts the degradation efficiency of BTEX in the process of O_3 alone. In this process, 26.81–40.71% of BTEXs were degraded in 60 min. Upon the combination of ozonation with single US of different frequency (i.e., 40, 80, 120, 200 kHz), the degradation efficiency of BTEX was evidently increased as illustrated in Fig. 3S. Specifically, the degradation rate of BTEXs was increased to 57.21–67.45% after 60 min with the combination of US-200 kHz with O_3. Although O_3 is a powerful oxidant with an oxidation potential of 2.08 V, the ozonation process of BTEX is limited due to the low direct reactivity and poor gas-liquid mass transfer rate (Gągol et al., 2018c; Bein et al., 2023). In US/O_3 processes, the rate of O_3 mass transfer is accelerated by the mechanical effects of US, such as turbulences and microcirculations providing greater mixing. Besides, O_3 undergoes thermal decomposition in the gaseous phase of cavitation bubbles yielding $HO^{\bullet}$ radicals *via* Eqs. 8, 9. The formation of $HO^{\bullet}$ radicals from H_2O is facilitated due the presence of highly reactive nascent oxygen atoms (Khan et al., 2023), which can also react with BTEXs. Consequently, these conversions contribute to the reduction of the dissolved O_3 concentration below the saturation value and promote the continuous diffusion of O_3 into the liquid. As a result, the combination of US and O_3 exhibited higher degradation efficiency of BTEX with respect to sole O_3.

$$O_3 \xrightarrow{cavitation} O_2 + O(^3P) \quad \text{Eq. 8}$$

$$O(^3P) + H_2O \xrightarrow{cavitation} HO^{\bullet} + HO^{\bullet} \quad \text{Eq. 9}$$

in order to demonstrate the effect of dual-frequency US on BTEX degradation by O_3, the ozonation was performed under the sonication of 40–120 kHz (LFDUS) and 80–200 kHz (HFDUS). As depicted in Fig. 3, the combined process of ozonation and LFDUS degraded 99.37–99.69% of BTEXs in 40 min. In contrast, the simultaneous operation of ozonation and HFDUS (Fig. 4) reached 86.09–91.76% of BTEX degradation after 60 min. The synergistic indexes determined according Eq. (7) were 7.86 and 2.9 for LFDUS/O_3 and HFDUS/O_3, respectively. These results indicated that the ozonation of BTEX in water can be significantly enhanced by application of dual-frequency US as the efficiency of both combined processes exceeded the cumulative effect of sole O_3 and DFUS.

The effectiveness of ozonation under US is generally attributed to the enhanced generation of $HO^{\bullet}$ radicals and reduced mass transfer

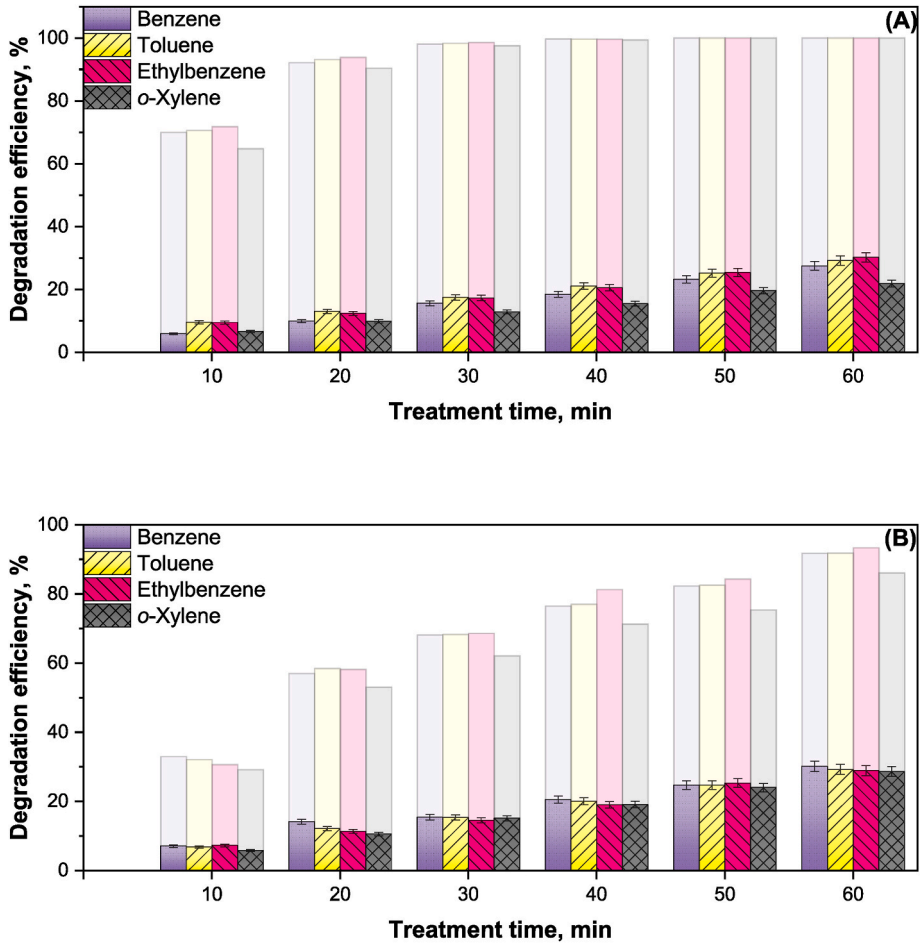

Fig. 7. Effect of NaN_3 on BTEX degradation in (a) LFDUS/O_3 and (b) HFDUS/O_3; $[BTEX]_0$: 50 ppm (v/v), $[O_3]$: $[NaN_3]$ = 1:10, pH 6.5, T = 20 ± 2.5 °C, O_3 flow rate 0.5 L min^{-1}, US: 600 W, 40/120 kHz (LFDUS) and 80/200 kHz (HFDUS). Shadowed data - corresponding processes without additives.

resistance. The enhanced degradation of pollutants in US/O_3 process is mainly caused by the accelerated generation of ROSs due to O_3 decomposition induced by collapse of cavitation bubbles (Chandak et al., 2020; Weavers et al., 1998; Ghanbari et al., 2020). The energy emitted during the collapse of cavitation bubbles, in turn, creates localized extreme conditions, so-called "hot spots", whereat O_3 undergo thermal decomposition (Gągol et al., 2018b, 2020). In such scenario, benzene, toluene, ethylbenzene, *o*-xylene with partition coefficient ($\log K_{ow}$) of 2.13, 2.73, 3.15 and 3.12, respectively, tend to diffuse to the interior and interfacial zones of the cavitation bubble. Inside the cavitating bubble, BTEXs are readily degraded *via* pyrolysis and oxidative degradation by a variety of generated ROSs at the interfacial zone.

Upon DFUS excitation, the steady-state oscillation of cavitation bubbles is disrupted and the evolution dynamics of cavitation bubbles is complex exhibiting unstable oscillation, which causes accelerated collapse of cavities (Ye et al., 2019). Importantly, the maximum radius and collapse pressure of cavitation bubbles in DFUS is significantly higher than that of obtained using single-frequency US at the same US power (Ye et al., 2019). Hence, the utilization of DFUS can disturb the treated solution more strongly and characterized by a high energy dissipation rate and cavitational yield compared to single-frequency US (Tatake and Pandit, 2002; Matafonova and Batoev, 2020; Zhang et al., 2017). Therefore, the formation of ROSs due to O_3 decomposition was increased in LDFUS/O_3 and HFDUS/O_3 resulting in high degradation efficiency of BTEX. As listed in Table 2, the degradation rate constant values of BTEX in LFDUS/O_3 were significantly higher than that of US/O_3-40 kHz and US/O_3-120 kHz. Since DFUS-assisted processes are electric-energy-intensive, the electric energy per order (E_{EO}) – electric energy required to degrade 90% of 1 m^3, 100 ppm BTEX solution were estimated. Taking into account the operating power of US reactor (0.3 kW for single-frequency US and 0.6 kW for dual-frequency) and O_3 generator (0.38 kW), the E_{EO} of LFDUS/O_3 was to 71.78 kW h m^{-3} $order^{-1}$, while single frequency US/O_3 processes at 40 and 120 kHz required 794.40 and 459.63 kW h m^{-3} $order^{-1}$, respectively. If the cost of energy is 0.17 USD per kWh for industrial customers in Poland, the treatment cost of BTEX in LFDUS/O_3 from electrical cost will be 7.9 USD m^{-3}. These observations highlight the superiority of DFUS over the single-frequency US in the ozonation of BTEX in water.

Taking into account that the decreased cavitation threshold is associated with a decrease in US frequency, the effect of the low frequency on cavitational events in DFUS is crucial (Matafonova and Batoev, 2020; Thanh Nguyen et al., 2017). It has been proposed that along with the generation of new cavitation nuclei, the low frequency US stimulates the diminishing of bubble interactions by the destruction of bubble clusters driven by high frequency US (Ciuti et al., 2000). Consequently, the application of low frequency US in DFUS increases the number of cavitation bubbles undergoing violent collapse and, thus, intensifies the cavitation events. With utilization of one low frequency US, high cavitation yields in DFUS were verified by measuring KI oxidation (Ebrahiminia et al., 2016), sonoluminescence generation (Ciuti et al., 2000) and H_2O_2 production (Lee and Oh, 2011). To date, the effectiveness of DFUS operated in the range of 20–176 kHz, 25–40 kHz and 30–50 kHz have been showed for the degradation of hexachlorobenzene (Hayashi et al., 2009), *p*-nitrophenol (Sivakumar et al., 2002) and formic acid (Gogate et al., 2003b), respectively. The results obtained in this study demonstrate that the combination of 40 kHz and 120 kHz (LDFUS/O_3)

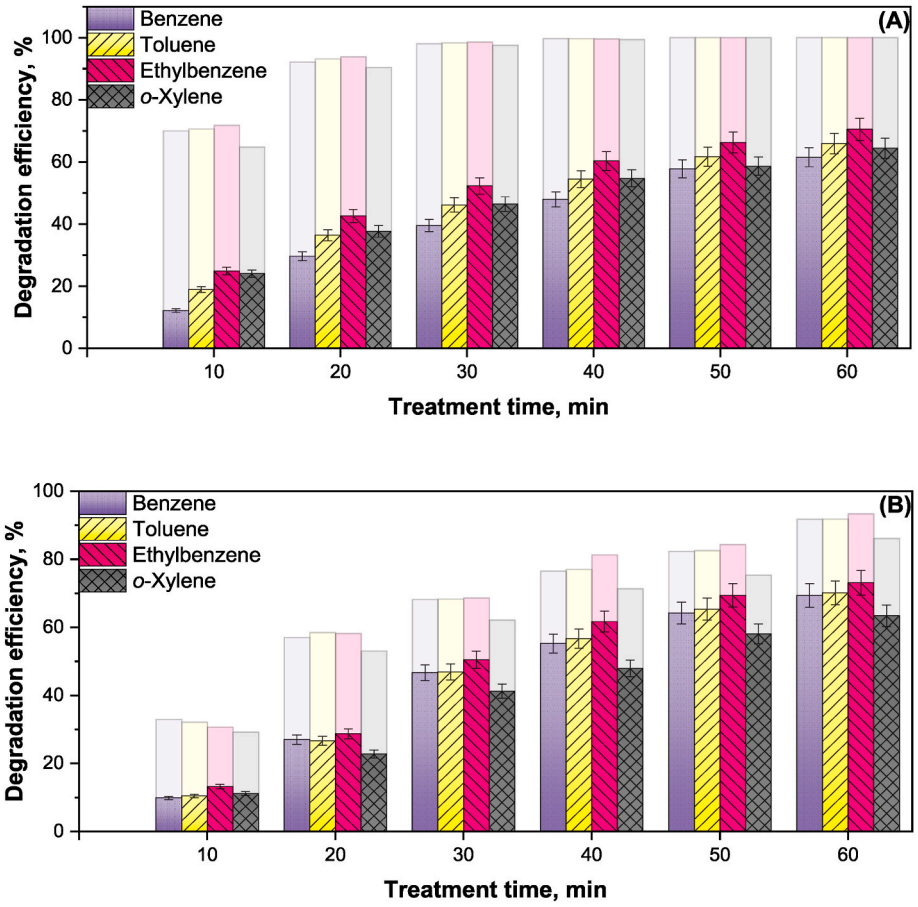

Fig. 8. Effect of *p*-BQ on BTEX degradation in (a) LFDUS/O_3 and (b) HFDUS/O_3; $[BTEX]_0$: 50 ppm (v/v), [O_3]: [*p*-BQ] = 1:10, pH 6.5, T = 20 ± 2.5 °C, O_3 flow rate 0.5 L min^{-1}, US: 600 W, 40/120 kHz (LFDUS) and 80/200 kHz (HFDUS). Shadowed data - corresponding processes without additives.

ensured a higher cavitation yield and generation of ROSs through O_3 decomposition, thereby providing higher degradation efficiency of BTEX. As listed in Table 2, the values of degradation rate constant of BTEX in LDFUS/O_3 were notably higher than those of HFDUS/O_3, which indicates the pivotal contribution of low-frequency US in sonochemical processes associated with acoustic cavitation.

3.3. Effect of pH

As a powerful oxidizing agent with oxidation potential of 2.08 V, O_3 is capable to degrade a variety of organic compounds or to convert them into easily biodegradable compounds. Based on pH of the reaction media, the oxidative degradation of pollutants proceeds through direct electrophilic attack by molecular O_3 or indirect pathway induced by ROSs from O_3 decomposition. To evaluate the effect of pH, BTEX degradation in LFDUS/O_3 and HFDUS/O_3 was performed at acidic and alkaline conditions. The pH study showed that BTEX degradation efficiency in both LFDUS/O_3 and HFDUS/O_3 systems was declined significantly at pH 3. Specifically, 18.78–31.88% of BTEXs were degraded by LFDUS/O_3 in 40 min (Fig. 5a). Similarly, the degradation efficiency of BTEXs in HFDUS/O_3 reached 28.18–32.59% in 60 min (Fig. 5b). The decreased degradation rate constants of BTEX observed at pH 3 (Table 3) suggested the predominance of direct pathway of oxidation by O_3. This is due to the low decomposition rate of O_3 at acidic pH and slow direct interaction of molecular O_3 with organic substrates. Interestingly, the degradation rate constants of ethylbenzene and *o*-xylene in LFDUS/O_3 and HFDUS/O_3 were decreased slightly compared to sole O_3, which can be related to the scavenging of $HO^\bullet$ radicals from **Eqs. 1 and 9** by O_3 with formation of hydroperoxyl radicals ($HO_2^\bullet$) with lower oxidation potential (Joseph et al., 2021):

$$HO^\bullet + O_3 \rightarrow HO_4^\bullet \; 2 \times 10^9 \; M^{-1}s^{-1} \quad \text{Eq. 10}$$

$$HO_4^\bullet \rightarrow HO_2^\bullet + O_2 \; 2.8 \times 10^4 \; M^{-1}s^{-1} \quad \text{Eq. 11}$$

The degradation of BTEX in LFDUS/O_3 and HFDUS/O_3 occurred faster upon the increase of pH to 11. Thus, 98.76, 99.22, 98.81, 96.71% of benzene, toluene, ethylbenzene and *o*-xylene, respectively, were degraded by LFDUS/O_3 in 60 min. Whereas, these pollutants were correspondingly degraded to 90.20, 89.80, 88.24 and 80.28%, respectively, in 60 min by HFDUS/O_3. At basic conditions, indirect oxidation of pollutants is the main route, as the dissolved O_3 undergoes decomposition to form highly reactive $HO^\bullet$ radicals responsible for degradation of contaminants:

$$O_3 + HO^- \rightarrow HO_2^- + O_2 \quad 40 \; M^{-1}s^{-1} \text{ at pH 10} \quad \text{Eq. 12}$$

$$HO_2^- + O_3 \rightarrow O_2^{\bullet -} + HO^\bullet + O_2 \; 5.5 \times 10^6 \; M^{-1}s^{-1} \quad \text{Eq. 13}$$

$$O_2^{\bullet -} + O_3 \rightarrow O_3^{\bullet -} + O_2 \; 1.6 \times 10^9 \; M^{-1}s^{-1} \quad \text{Eq. 14}$$

$$O_3^{\bullet -} + H_2O \rightarrow HO^\bullet + HO^- + O_2 \; 9.4 \times 10^7 \; M^{-1}s^{-1} \quad \text{Eq. 15}$$

Despite the effective conversion of O_3 to $HO^\bullet$ radicals at basic pH, the degradation rate constants were increased only for benzene and ethylbenzene in HFDUS/O_3 at pH 11 in 60 min, while the corresponding *k* values of BTEX in LFDUS/O_3 were lower compared to pH 6.5 (Table 3). Such effect could be related to the reduced amount of $HO^\bullet$ radicals generated in the gas phase of cavitation bubbles, where hydrophobic BTEXs are degraded. In contrast, the alkaline reaction medium

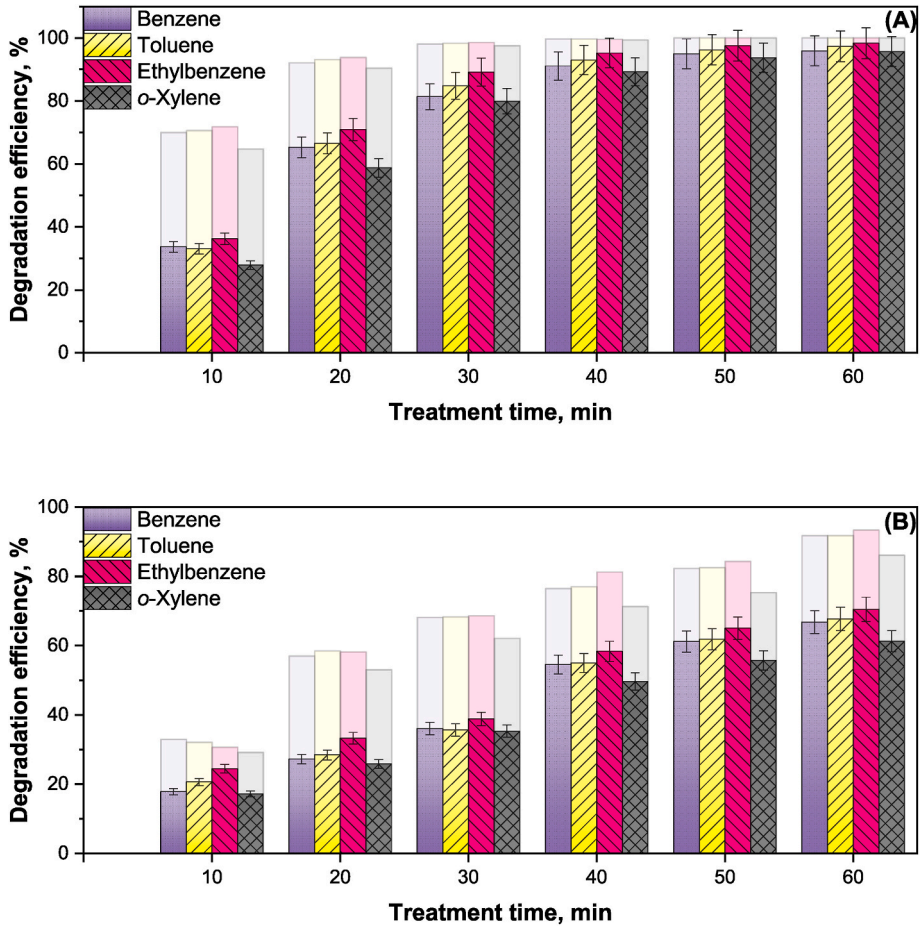

Fig. 9. The effect of Cl^- on BTEX degradation in (a) LFDUS/O_3 and (b) HFDUS/O_3; $[BTEX]_0$: 50 ppm (v/v), [O_3]: [NaCl] = 1:10, pH 6.5, T = 20 ± 2.5 °C, O_3 flow rate 0.5 L min^{-1}, US: 600 W, 40/120 kHz (LFDUS) and 80/200 kHz (HFDUS). Shadowed data - corresponding processes without additives.

competitively consumed the dissolved O_3, thereby increasing the fraction of $HO^•$ radicals in the bulk liquid. Since, the effectiveness of LFDUS/O_3 and HFDUS/O_3 was not improved significantly with the increase of pH, further experiments were conducted without pH adjustment.

3.4. Identification of ROSs

Besides primary $HO^•$ radicals, the decomposition of O_3 can lead to the formation of secondary reactive radicals such as superoxide ($O_2^{•-}$) radicals and singlet oxygen ($^1O_2$), which also contribute to the degradation of contaminants. The formation of $O_2^{•-}$ radicals is known to occur during the decomposition of O_3 in water at acidic to neutral conditions, while $^1O_2$ is considered to derive from radical recombination reactions (Joseph et al., 2021; Kasprzyk-Hordern et al., 2003; Nan et al., 2024) (**Eqs. (16)–(18)**) In order to evaluate the contribution of ROSs in LFDUS/O_3 and HFDUS/O_3, a series of quenching experiments were conducted. Owing to its high reactivity with $HO^•$ radicals (9.7×10^8 M^{-1} s^{-1}), methanol (MeOH) was employed to quench $HO^•$ radicals, while $O_2^{•-}$ radicals were quenched by *para*-benzoquinone (*p*-BQ) with a rate constant of 1.0×10^9 $M^{-1}s^{-1}$ (Rao and Hayon, 1975; Buxton et al., 1988). Sodium azide (NaN_3) with a rate constant of $\sim 10^8$ $M^{-1}s^{-1}$ was used to verify the presence of $^1O_2$ (Wang and Wang, 2020).

$$O_3 + HO^- \rightarrow O_2^{•-} + HO_2^• \quad 70\ M^{-1}s^{-1} \qquad \text{Eq. 16}$$

$$O_2^{•-} + HO^• \rightarrow {}^1O_2 + HO^- \qquad \text{Eq. 17}$$

$$O_2^{•-} + O_2^{•-} + 2H^+ \rightarrow {}^1O_2 + H_2O_2 \qquad \text{Eq. 18}$$

As presented in Fig. 6a and b, MeOH effectively inhibited BTEX degradation in both LFDUS/O_3 and HFDUS/O_3 processes. After 40 min of treatment only 42.3–45.7 % of BTEXs were degraded in LFDUS/O_3 in the presence of MeOH. On the other hand, the degradation efficiency of HFDUS/O_3 was decreased to 41.2–55.6 % after 60 min of treatment. Obtained results suggest $HO^•$ radicals as predominant species participating in the radical-induced oxidation of BTEX in LFDUS/O_3 and HFDUS/O_3. The BTEXs degradation rate constant values determined in the presence of MeOH in LFDUS/O_3 (Table 4) were decreased in approx. 90.2% compared to LFDUS/O_3 without scavengers. In the case of HFDUS/O_3, a trend of *k* decrease by the addition of MeOH was ~68%. These observations suggested that the impact of $HO^•$ radicals towards BTEX degradation was higher in LFDUS/O_3 compared to HFDUS/O_3.

On the other hand, as shown in Fig. 7a, the degradation efficiency of BTEXs was significantly suppressed by 78.6–83.9%, respectively for 40 min of treatment with the addition of NaN_3 in LFDUS/O_3. The presence of NaN_3 correspondingly inhibited the efficacy of HFDUS/O_3 by 57.4–64% in 60 min (Fig. 7b). According to literature, NaN_3 reacts with $HO^•$ and O_3 with rate constants of 1.2×10^{10} $M^{-1}s^{-1}$ and 2.5×10^6 $M^{-1}s^{-1}$, respectively (Betterton and Craig, 1999; Sun et al., 2021). Thus, the inhibitory effect of NaN_3 observed in this study can be attributed to the impact of both $HO^•$ radicals and $^1O_2$. Taking into account that MeOH verified the presence of $HO^•$ radicals in LFDUS/O_3 and HFDUS/O_3, it can be assumed that both $HO^•$ radicals and $^1O_2$ were involved in BTEX degradation, whereat $^1O_2$ played a minor role. In addition, degradation rate constant of BTEX in LFDUS/O_3 (Table 4) was suppressed in lower extend in the presence of MeOH as compared to HFDUS/O_3, while the rate constants obtained with addition of NaN_3 were similar. These findings may imply that Eqs. (17) and (18) were significant in larger

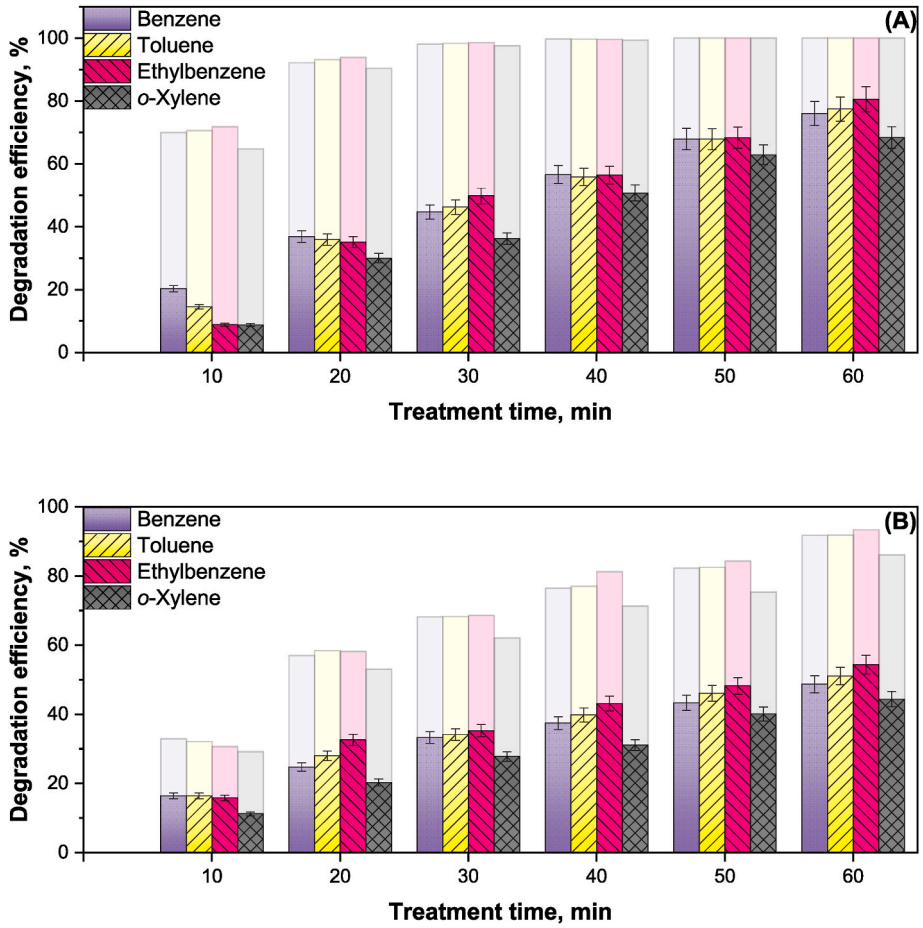

Fig. 10. The effect of SO_4^{2-} on BTEX degradation in (a) LFDUS/O_3 and (b) HFDUS/O_3; $[BTEX]_0$: 50 ppm (v/v), $[O_3]$: $[Na_2SO_4]$ = 1:10, pH 6.5, T = 20 ± 2.5 °C, O_3 flow rate 0.5 L min^{-1}, US: 600 W, 40/120 kHz (LFDUS) and 80/200 kHz (HFDUS). Shadowed data - corresponding processes without additives.

cavitation bubbles with longer collapse time generated in LFDUS/O_3.

As depicted in Fig. 8a and b, the addition of *p*-BQ inhibited the degradation efficiency of BTEX in both LFDUS/O_3 and HFDUS/O_3. The degradation efficiency of benzene, toluene, ethylbenzene, *o*-xylene with addition of *p*-BQ were 61.50, 65.88, 70.49, and 64.42%, respectively, after 60 min of treatment by LFDUS/O_3. As shown in Fig. 8b, HFDUS/O_3/*p*-BQ degraded 69.34, 70.11, 73.05, 63.36%, of benzene, toluene, ethylbenzene and *o*-xylene in 60 min, respectively. Since *p*-BQ can also partially quench $HO^•$ radicals (6.6×10^9 $M^{-1}s^{-1}$) (Fónagy et al., 2021), these results are discussed to confirm the involvement of $O_2^{•-}$ radicals in BTEX degradation. To conclude, it can be proposed that $HO^•$ radicals were the main reactive species responsible for the degradation of BTEX in LFDUS/O_3 and HFDUS/O_3, while $O_2^{•-}$ radicals and $^1O_2$ played a minor role.

3.5. Effect of co-existing inorganic anions

Practical implementation of novel chemical processes in water treatment strategies presumes operations with natural water containing a variety of constituents, such as natural organic matter (NOM), co-existing inorganic anions, mineral cations etc. In order to determine the effect of inorganic anions, the degradation of BTEX by LFDUS/O_3 and HFDUS/O_3 was performed in the presence of chloride (Cl^-), carbonate (CO_3^{2-}) and sulfate anions (SO_4^{2-}). Fig. 9a and b illustrate the degradation efficiency of BTEX during LFDUS/O_3 and HFDUS/O_3 in presence of Cl^- anions. It can be seen that the addition of Cl^- anions had an adverse effect on BTEX degradation in both processes. The degradation efficiency was reduced by 4.35–10.1% after 40 min in LFDUS/O_3. However, still the performance of the processes was on acceptable level.

Scavenging effect of Cl^- anions on BTEX degradation was more pronounced in HFDUS/O_3 (Fig. 9b). Degradation rates of BTEXs were reduced by 22.89–24.95%, respectively, after 60 min of treatment. The inhibitory effect of Cl^- anions is commonly attributed to the scavenging of $HO^•$ radicals to form chlorine oxidizers (i.e., $Cl^•$, $Cl_2^{•-}$ and $HClO^{•-}$) with lower oxidation potential (**Eqs. (19)–(21)**) (von Gunten, 2003; Asghar et al., 2022). However, the sequence of radical reactions initiated with **Eq. (19)** is pH-depended and the steady-state concentration of $HOCl^{•-}$ at neutral conditions is negligible as the reverse reaction with 6.1×10^9 M^{-1} s^{-1} prevails (Yu and Barker, 2003). Thus, the inhibitory effect of Cl^- anions can be referred to the direct competitive reaction with O_3 to yield OCl^- (**Eq. (22)**), which is present in equilibrium with HOCl at neutral conditions and stable to O_3 oxidation (Asghar et al., 2022).

$$Cl^- + HO^• \leftrightarrow HOCl^{•-}\ 4.3 \times 10^9\ M^{-1}\ s^{-1} \quad \text{Eq. 19}$$

$$HOCl^{•-} + H^+ \rightarrow Cl^• + H_2O\ 2 \times 10^{10}\ M^{-1}\ s^{-1} \quad \text{Eq. 20}$$

$$Cl^• + Cl^- \rightarrow Cl_2^{•-}\ 7.8 \times 10^9\ M^{-1}\ s^{-1} \quad \text{Eq. 21}$$

$$Cl^- + O_3 \rightarrow OCl^- + O_2 \quad \text{Eq. 22}$$

$$OCl^- \leftrightarrow HOCl\ pK_a\ 7.5 \quad \text{Eq. 23}$$

As shown in Fig. 10a and b, SO_4^{2-} anions caused the reduction of BTEX degradation efficiency in both LFDUS/O_3 and HFDUS/O_3 processes. SO_4^{2-} anions are commonly considered as a scavenger of $HO^•$ radicals due to inevitable generation of $SO_4^{•-}$ radicals (**Eq. (24)**) (Dehvari et al., 2020; Golshan et al., 2018). The degradation efficiency of BTEX in LFDUS/O_3 and HFDUS/O_3 was decreased as SO_4^{2-} anions partially

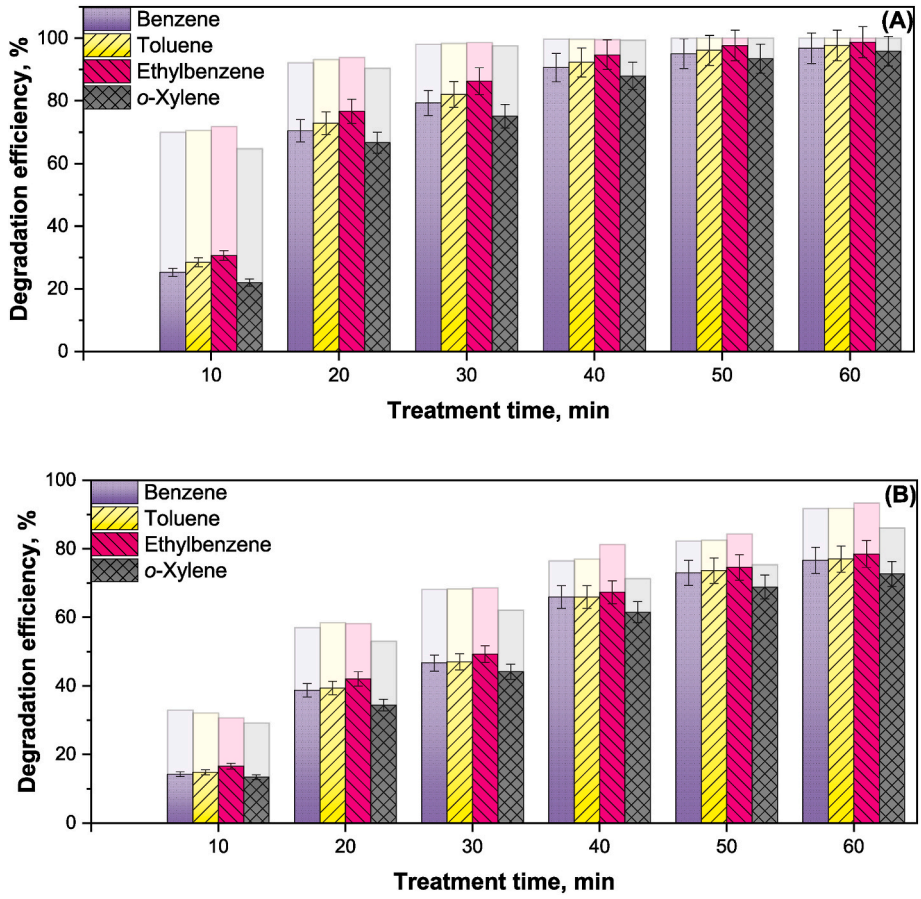

Fig. 11. The effect of CO_3^{2-} on BTEX degradation in (a) LFDUS/O_3 and (b) HFDUS/O_3; $[BTEX]_0$: 50 ppm (v/v), $[O_3]$: $[Na_2CO_3]$ = 1:10, pH 10.5, T = 20 ± 2.5 °C, O_3 flow rate 0.5 L min^{-1}, US: 600 W, 40/120 kHz (LFDUS) and 80/200 kHz (HFDUS). Shadowed data - corresponding processes without additives.

Table 5
Pseudo-first-order kinetic model parameters of BTEX degradation in LFDUS/O_3 and HFDUS/O_3 systems in the presence of inorganic anions.

Anion	Process	Benzene	Toluene	Ethylbenzene	*o*-Xylene
		k, min^{-1}	*k*, min^{-1}	*k*, min^{-1}	*k*, min^{-1}
Cl^-	LFDUS/O_3	0.0575	0.0649	0.0738	0.0560
	HFDUS/O_3	0.0188	0.0190	0.0203	0.0160
SO_4^{2-}	LFDUS/O_3	0.0231	0.0242	0.0265	0.0200
	HFDUS/O_3	0.0106	0.0114	0.0125	0.0096
CO_3^{2-}	LFDUS/O_3	0.0602	0.0656	0.0760	0.0555
	HFDUS/O_3	0.0259	0.0262	0.0270	0.0231

consumed $HO^\bullet$ radicals and formed $SO_4^{\bullet-}$ radicals possess relatively lower oxidation potential (2.5–3.1 V) and selectivity towards electron-rich substances (Tian et al., 2022). Particularly, the presence SO_4^{2-} anions in LFDUS/O_3 suppressed the degradation efficiency of BTEXs by 43.1–48.7%, in 40 min of the treatment. In the case of HFDUS/O_3, the degradation efficiency of these compounds was correspondingly reduced by 40.7–43.04% after 60 min.

$$HO^\bullet + SO_4^{2-} \rightarrow SO_4^{\bullet-} + HO^- \quad \text{Eq. 24}$$

As shown in Fig. 11a and b, the addition of CO_3^{2-} anions demonstrated negligible inhibitory effect on BTEX degradation in both LFDUS/O_3 and HFDUS/O_3 processes. With the addition of CO_3^{2-} anions, the degradation efficiency was declined by 4.9–11.4% in LFDUS/O_3, respectively, in 40 min. The corresponding inhibitory effect of CO_3^{2-} anions in HFDUS/O_3 after 60 min was a bit higher – a 13.4–15.1% decrease was observed. This effect is conditioned by the dual impact of CO_3^{2-} anions, which is comprised of two contrary factors. Firstly, CO_3^{2-} anions are strong scavengers of $HO^\bullet$ radicals forming $CO_3^{\bullet-}$ radicals (**Eq. (25)**) with lower oxidation potential and selectivity towards certain contaminants (Gągol et al., 2020; Kasprzyk-Hordern et al., 2003; Rayaroth et al., 2023). Secondly, addition of CO_3^{2-} anions lead to the increase of pH. Strong alkaline condition (pH~11.0) facilitates O_3 decomposition resulting in generation of $HO^\bullet$ radicals (Gągol et al., 2018c). As was discussed in **section 3.3**, such conversion takes place in the bulk liquid phase, while the degradation of BTEX proceeds in the gaseous phase of cavitation bubbles. Hence, the base-catalyzed decomposition of O_3 led to the accumulation of $HO^\bullet$ radicals in bulk liquid thereby hindering the efficient utilization of O_3 for BTEX degradation under cavitation.

$$HO^\bullet + CO_3^{2-} \rightarrow CO_3^{\bullet-} + HO^- \; 4.2 \times 10^8 \; M^{-1}s^{-1} \quad \text{Eq. 25}$$

The degradation rate constants of BTEX in LFDUS/O_3 and HFDUS/O_3 determined in the presence of co-existing anions are presented in Table 5. According to obtained results, the negative impact of inorganic anions showed the following order: $SO_4^{2-} > Cl^- > CO_3^{2-}$ in both LFDUS/O_3 and HFDUS/O_3 processes. The inhibitory effect of inorganic anions on degradation of organic contaminants may be considerable when LFDUS/O_3 and HFDUS/O_3 processes are applied in the treatment of real wastewater effluents.

3.6. *Identification of intermediates and possible degradation mechanism*

Inefficient AOPs often lead to the incomplete mineralization of organic pollutants. Therefore, such processes are related with the formation of undesirable degradation intermediates. These intermediates may pose the toxicity risk greater than parent contaminants causing

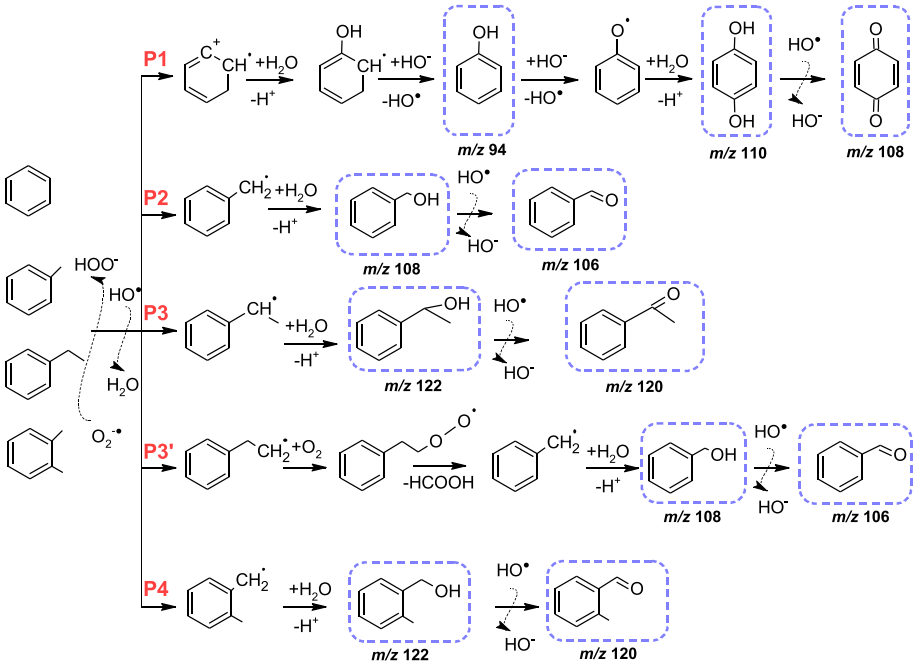

Fig. 12. The proposed degradation mechanism of BTEX in LFDUS/O_3 and HFDUS/O_3.

secondary pollution. In order to reveal the intermediates of BTEX degradation in LFDUS/O_3 and HFDUS/O_3 processes, treated samples of BTEX at certain time interval were analyzed by GC-MS. The intermediates were identified using SCAN mode based on the peak analysis performed by similarity search. The possible degradation mechanism of BTEX was proposed based on the identified intermediates. To elucidate the individual degradation product of each BTEX component, model solutions of benzene, toluene, ethylbenzene and *o*-xylene were separately treated by LFDUS/O_3 and HFDUS/O_3. These model solutions of benzene, toluene, ethylbenzene, *o*-xylene were prepared with the concentration of 800 ppm, 450 ppm, 300 ppm and 250 ppm, respectively, for better expression of intermediate peaks in GC-MS chromatogram to ease the detection.

Generally, oxidative degradation of organic contaminants during ozonation under US is conducted by ROSs, such as $HO^{\bullet}$, $O_2^{\bullet-}$, $^1O_2$. In this case, aromatic hydrocarbons react with ROSs *via* hydrogen abstraction (H-abstraction) from benzoic ring or methyl/ethyl groups of aromatic compounds. Oxidation intermediates may further undergo hydroxylation, dealkylation and consecutive mineralization. As shown in Table S1, several intermediates were detected during oxidative degradation of BTEX. Specifically, phenol, hydroquinone and *p*-benzoquinone were formed during benzene degradation. Toluene was accordingly converted to benzyl alcohol and benzaldehyde, while 1-phenylethanol, acetophenone, benzene alcohol, benzaldehyde, *o*-methylbenzyl alcohol and *o*-tolualdehyde were present in treated samples of ethylbenzene and *o*-xylene.

Based on the range of detected intermediates, it can be suggested that the oxidative degradation of benzene was processed *via* the radical route in both LFDUS/O_3 and HFDUS/O_3 processes. When benzene reacts with $HO^{\bullet}$/$O_2^{\bullet-}$ radicals, the aromatic ring undergoes H-abstraction to form a cation radical. The cation radicals can react with H_2O resulting to OH-group addition with further propagation of the radical adduct yielding phenol (m/z 94). Detection of hydroquinone (m/z 110) and *p*-benzoquinone (m/z 108) suggests the hydroxylation of phenol in *para*-position and subsequent re-arrangement of conjugated π-π system. H-abstraction of toluene, ethylbenzene and *o*-xylene proceeded from alkyl groups attached to the aromatic ring as C–H bond energy in alkyl groups is lower than in the aromatic ring. Initiated by H-abstraction, the radical route of oxidation involves several steps, possibly including hydroxylation and dealkylation prior to ring-opening reactions. As illustrated in Fig. 12, the primary step of toluene degradation started with H-abstraction from methyl group by $HO^{\bullet}$ or $O_2^{\bullet-}$ radicals. The obtained radical adduct underwent hydroxylation in presence of water and readily oxidized by ROSs to form benzyl alcohol (m/z 108) and benzaldehyde (m/z 106). These intermediates were also detected in treated samples of ethylbenzene implying the dealkylation of ethyl group, which is possible with elimination of formic acid in presence of oxygen. Then, the obtained aromatic radical repeated the degradation pathway described for toluene. Additionally, non-selective attack of ROSs caused β-H-abstraction from ethylbenzene resulting in formation of 1-phenylethanol (m/z 122) and acetophenone (m/z 120). In case of *o*-xylene, H-abstraction can be conducted from one of the methyl groups. Identification of *o*-methylbenzyl alcohol (m/z 122) and *o*-tolualdehyde (m/z 120) in the treated solution reflects the consecutive hydroxylation and oxidation of one methyl group of *o*-xylene. These intermediates were not detected in final samples of studied processes (detection limits for such VOCs for used DLLME-GC-MS based method are below 5 ppb (Makoś et al., 2018)) for primary concentration of BTEXs 50 ppms confirming their further complete degradation.

4. Conclusions

The oxidative degradation of BTEX in US/O_3 was significantly enhanced by the introduction of the second source of US. The combination of O_3 and dual-frequency US with operating frequencies of 40 and 120 kHz (LFDUS/O_3) exhibited higher degradation capacity than 80/200 kHz US (HFDUS/O_3). Both combined processes could effectively degrade BTEX at pH 6.5, O_3 containing gas flow rate 0.5 L min^{-1}, US power input 600 W, frequencies: 40/120 kHz for LFDUS and 80/200 kHz for HFDUS, respectively. The synergistic indexes of 1.13 and 0.94 were obtained for BTEX degradation in LFDUS and HFDUS, respectively. The combination of LFDUS and HFDUS with O_3 resulted in significant increase of BTEX degradation efficiency with the synergistic indexes of 7.86 and 2.9, respectively. Synergistic effect for LFDUS is unusual and largely exceeds typically reported values of synergistic coefficient available in the literature (typically not higher than 4.0). The observed results confirmed the crucial role of dual-frequency US for specific and not obvious frequency values in acoustic cavitation, which contributes

to sonochemical generation of $HO^{\bullet}$ radicals and O_3 decomposition. The presence of SO_4^{2-} and Cl^- anions noticeably inhibited the degradation efficiency of BTEX in LFDUS/O_3 and HFDUS/O_3, whereas CO_3^{2-} showed negligible inhibitory effect. Also in this aspect LFDUS revealed to be more effective and stable under simulated real conditions. Quenching experiments indicated that $HO^{\bullet}$ radicals were the dominant reactive species responsible for BTEX degradation, singlet oxygen also importantly contributed in degradation, while $O_2^{\bullet-}$ radicals had a minor contribution. Identification of degradation intermediates using GC-MS confirmed the radical route of BTEX oxidation in LFDUS/O_3 and HFDUS/O_3. The study contributes to the understanding of hybrid cavitation-based AOPs for the removal of water contaminants emphasizing the importance of process parameters and water constituents on the removal efficiency. As a part of ongoing trend towards environmental sustainability, future research can focus on scaling up LFDUS/O_3 and HFDUS/O_3 processes for the treatment of real wastewaters. In case of the developed process, increase of the treatment scale seems possible, as both ozonation and ultrasonic systems are already available for industrial scale processes.

CRediT authorship contribution statement

Kirill Fedorov: Writing – original draft, Visualization, Methodology, Investigation, Conceptualization. **Lingshuai Kong:** Writing – review & editing, Validation. **Chongqing Wang:** Writing – review & editing, Validation. **Grzegorz Boczkaj:** Writing – review & editing, Writing – original draft, Validation, Supervision, Resources, Project administration, Methodology, Funding acquisition, Conceptualization.

Declaration of competing interest

The authors declare that they have no known competing financial interests or personal relationships that could have appeared to influence the work reported in this paper.

Data availability

No data was used for the research described in the article.

Acknowledgements

The authors gratefully acknowledge financial support from the National Science Centre, Warsaw, Poland for project OPUS nr UMO-2017/25/B/ST8/01364.

Appendix A. Supplementary data

Supplementary data to this article can be found online at https://doi.org/10.1016/j.jenvman.2024.121343.

References

Adewuyi, Y.G., 2001. Sonochemistry: environmental science and engineering applications. Ind. Eng. Chem. Res. 40, 4681–4715. https://doi.org/10.1021/ie010096l.

Al-Harbi, M., 2019. Characteristic of atmospheric BTEX concentrations and their health implications in urban environment. Appl. Ecol. Environ. Res. 17, 33–51.

Ammar, H.B., 2016. Sono-Fenton process for metronidazole degradation in aqueous solution: effect of acoustic cavitation and peroxydisulfate anion. Ultrason. Sonochem. https://doi.org/10.1016/j.ultsonch.2016.04.035.

Asghar, A., V Lutze, H., Tuerk, J., Schmidt, T.C., 2022. Influence of water matrix on the degradation of organic micropollutants by ozone based processes: a review on oxidant scavenging mechanism. J. Hazard Mater. 429, 128189 https://doi.org/10.1016/j.jhazmat.2021.128189.

Beckett, M.A., Hua, I., 2000. Elucidation of the 1,4-dioxane decomposition pathway at discrete ultrasonic frequencies. Environ. Sci. Technol. 34, 3944–3953. https://doi.org/10.1021/es000928r.

Bein, E., Seiwert, B., Reemtsma, T., Drewes, J.E., Hübner, U., 2023. Advanced oxidation processes for removal of monocyclic aromatic hydrocarbon from water: effects of O3/H2O2 and UV/H2O2 treatment on product formation and biological post-treatment. J. Hazard Mater. 450, 131066 https://doi.org/10.1016/J.JHAZMAT.2023.131066.

Betterton, E.A., Craig, D., 1999. Kinetics and mechanism of the reaction of azide with ozone in aqueous solution. J. Air Waste Manage. Assoc. 49, 1347–1354. https://doi.org/10.1080/10473289.1999.10463958.

Boczkaj, G., Makoś, P., Przyjazny, A., 2016a. Application of dispersive liquid–liquid microextraction and gas chromatography with mass spectrometry for the determination of oxygenated volatile organic compounds in effluents from the production of petroleum bitumen. J. Separ. Sci. https://doi.org/10.1002/jssc.201501355.

Boczkaj, G., Makoś, P., Fernandes, A., Przyjazny, A., 2016b. New procedure for the control of the treatment of industrial effluents to remove volatile organosulfur compounds. J. Separ. Sci. https://doi.org/10.1002/jssc.201600608.

Boczkaj, G., Makoś, P., Fernandes, A., Przyjazny, A., 2017. New procedure for the examination of the degradation of volatile organonitrogen compounds during the treatment of industrial effluents. J. Separ. Sci. https://doi.org/10.1002/jssc.201601237.

Buxton, G.V., Greenstock, C.L., Helman, W.P., Ross, A.B., 1988. Critical Review of rate constants for reactions of hydrated electrons, hydrogen atoms and hydroxyl radicals (·OH/·O $^-$ in Aqueous Solution. J. Phys. Chem. Ref. Data 17, 513–886. https://doi.org/10.1063/1.555805.

Cako, E., Gunasekaran, K.D., Cheshmeh Soltani, R.D., Boczkaj, G., 2020. Ultrafast degradation of brilliant cresyl blue under hydrodynamic cavitation based advanced oxidation processes (AOPs). Water Resour. Ind. https://doi.org/10.1016/j.wri.2020.100134.

Carneiro, P.M., Firmino, P.I.M., Costa, M.C., Lopes, A.C., dos Santos, A.B., 2014. Multivariate optimization of headspace-GC for the determination of monoaromatic compounds (benzene, toluene, ethylbenzene, and xylenes) in waters and wastewaters. J. Separ. Sci. 37, 265–271. https://doi.org/10.1002/jssc.201300668.

Chandak, S., Ghosh, P.K., Gogate, P.R., 2020. Treatment of real pharmaceutical wastewater using different processes based on ultrasound in combination with oxidants. Process Saf. Environ. Protect. 137, 149–157. https://doi.org/10.1016/j.psep.2020.02.025.

Ciuti, P., Dezhkunov, N.V., Francescutto, A., Kulak, A.I., Iernetti, G., 2000. Cavitation activity stimulation by low frequency field pulses. Ultrason. Sonochem. https://doi.org/10.1016/S1350-4177(99)00037-1.

Dehvari, M., Ghanbari, F., Ahmadi, M., 2020. Sonochemical degradation of bisphenol A using persulfate activated by hematite nanoparticles. Water Sci. Technol. 83, 567–579. https://doi.org/10.2166/wst.2020.592.

Durmusoglu, E., Taspinar, F., Karademir, A., 2010. Health risk assessment of BTEX emissions in the landfill environment. J. Hazard Mater. 176, 870–877. https://doi.org/10.1016/j.jhazmat.2009.11.117.

Ebrahiminia, A., Mokhtari-Dizaji, M., Toliyat, T., 2016. Dual frequency cavitation event sensor with iodide dosimeter. Ultrason. Sonochem. 28, 276–282. https://doi.org/10.1016/J.ULTSONCH.2015.07.005.

Emmanuel, S.S., Olawoyin, C.O., Ayodele, I.D., Oluwole, O.J., 2023. Emerging nanosemiconductors for photocatalytic degradation of mono-aromatic volatile organic compounds (BTEX): a pragmatic review. J. Organomet. Chem. 996, 122767 https://doi.org/10.1016/J.JORGANCHEM.2023.122767.

Fedorov, K., Plata-Gryl, M., Khan, J.A., Boczkaj, G., 2020. Ultrasound-assisted heterogeneous activation of persulfate and peroxymonosulfate by asphaltenes for the degradation of BTEX in water. J. Hazard Mater. 397, 122804 https://doi.org/10.1016/j.jhazmat.2020.122804.

Feng, R., Zhao, Y., Zhu, C., Mason, T.J., 2002. Enhancement of ultrasonic cavitation yield by multi-frequency sonication. Ultrason. Sonochem. 9, 231–236. https://doi.org/10.1016/S1350-4177(02)00083-4.

Fitzgerald, M.E., Griffing, V., Sullivan, J., 2004. Chemical effects of Ultrasonics—"Hot spot" chemistry. J. Chem. Phys. 25, 926–933. https://doi.org/10.1063/1.1743145.

Fónagy, O., Szabó-Bárdos, E., Horváth, O., 2021. 1,4-Benzoquinone and 1,4-hydroquinone based determination of electron and superoxide radical formed in heterogeneous photocatalytic systems. J. Photochem. Photobiol. Chem. 407, 113057 https://doi.org/10.1016/J.JPHOTOCHEM.2020.113057.

Gągol, M., Przyjazny, A., Boczkaj, G., 2018a. Effective method of treatment of industrial effluents under basic pH conditions using acoustic cavitation – a comprehensive comparison with hydrodynamic cavitation processes. Chem. Eng. Process. - Process Intensif. 128, 103–113. https://doi.org/10.1016/j.cep.2018.04.010.

Gągol, M., Przyjazny, A., Boczkaj, G., 2018b. Wastewater treatment by means of advanced oxidation processes based on cavitation – a review. Chem. Eng. J. 338, 599–627. https://doi.org/10.1016/j.cej.2018.01.049.

Gągol, M., Przyjazny, A., Boczkaj, G., 2018c. Highly effective degradation of selected groups of organic compounds by cavitation based AOPs under basic pH conditions. Ultrason. Sonochem. 45, 257–266. https://doi.org/10.1016/j.ultsonch.2018.03.013.

Gągol, M., Soltani, R.D.C., Przyjazny, A., Boczkaj, G., 2019. Effective degradation of sulfide ions and organic sulfides in cavitation-based advanced oxidation processes (AOPs). Ultrason. Sonochem. 58, 104610 https://doi.org/10.1016/J.ULTSONCH.2019.05.027.

Gągol, M., Cako, E., Fedorov, K., Soltani, R.D.C., Przyjazny, A., Boczkaj, G., 2020. Hydrodynamic cavitation based advanced oxidation processes: studies on specific effects of inorganic acids on the degradation effectiveness of organic pollutants. J. Mol. Liq. 307 https://doi.org/10.1016/j.molliq.2020.113002.

Ghanbari, F., Khatebasreh, M., Mahdavianpour, M., Lin, K.Y.A., 2020. Oxidative removal of benzotriazole using peroxymonosulfate/ozone/ultrasound: synergy, optimization, degradation intermediates and utilizing for real wastewater. Chemosphere. https://doi.org/10.1016/j.chemosphere.2019.125326.

Gogate, P.R., Mujumdar, S., Pandit, A.B., 2003a. Large-scale sonochemical reactors for process intensification: design and experimental validation. J. Chem. Technol. Biotechnol. https://doi.org/10.1002/jctb.697.
Gogate, P.R., Mujumdar, S., Pandit, A.B., 2003b. Sonochemical reactors for waste water treatment: comparison using formic acid degradation as a model reaction. Adv. Environ. Res. 7, 283–299. https://doi.org/10.1016/S1093-0191(01)00133-2.
Golshan, M., Kakavandi, B., Ahmadi, M., Azizi, M., 2018. Photocatalytic activation of peroxymonosulfate by TiO2 anchored on cupper ferrite (TiO2@CuFe2O4) into 2,4-D degradation: process feasibility, mechanism and pathway. J. Hazard Mater. 359, 325–337. https://doi.org/10.1016/J.JHAZMAT.2018.06.069.
Guo, H., Lee, S.C., Chan, L.Y., Li, W.M., 2004. Risk assessment of exposure to volatile organic compounds in different indoor environments. Environ. Res. https://doi.org/10.1016/S0013-9351(03)00035-5.
Hashemi, S.H., Kaykhaii, M., Mirmoghaddam, M., Boczkaj, G., 2020. Preconcentration and analytical methods for determination of methyl tert-butyl ether and other fuel oxygenates and their degradation products in environment: a review. Crit. Rev. Anal. Chem. https://doi.org/10.1080/10408347.2020.1753164.
Hayashi, N., Liang, J., Choshi, H., Kasai, E., 2009. Hexachlorobenzene removal from a model sediment by using ultrasonic irradiation. Water Sci. Technol. 59, 737–744. https://doi.org/10.2166/wst.2009.021.
Hazrati, S., Rostami, R., Farjaminezhad, M., Fazlzadeh, M., 2016. Preliminary assessment of BTEX concentrations in indoor air of residential buildings and atmospheric ambient air in Ardabil, Iran. Atmos. Environ. 132, 91–97. https://doi.org/10.1016/j.atmosenv.2016.02.042.
Hua, I., Hochemer, R.H., Hoffmann, M.R., 1995. Sonochemical degradation of p-nitrophenol in a parallel-plate near-field acoustical processor. Environ. Sci. Technol. 29, 2790–2796.
Jawale, R.H., Gogate, P.R., 2018. Combined treatment approaches based on ultrasound for removal of triazophos from wastewater. Ultrason. Sonochem. https://doi.org/10.1016/j.ultsonch.2017.02.019.
Joseph, C.G., Farm, Y.Y., Taufiq-Yap, Y.H., Pang, C.K., Nga, J.L.H., Li Puma, G., 2021. Ozonation treatment processes for the remediation of detergent wastewater: a comprehensive review. J. Environ. Chem. Eng. 9, 106099 https://doi.org/10.1016/J.JECE.2021.106099.
Kamal, M.S., Razzak, S.A., Hossain, M.M., 2016. Catalytic oxidation of volatile organic compounds (VOCs) - a review. Atmos. Environ. https://doi.org/10.1016/j.atmosenv.2016.05.031.
Kasprzyk-Hordern, B., Ziółek, M., Nawrocki, J., 2003. Catalytic ozonation and methods of enhancing molecular ozone reactions in water treatment. Appl. Catal. B Environ. 46, 639–669. https://doi.org/10.1016/S0926-3373(03)00326-6.
Khan, F.I., Ghoshal, A. Kr, 2000. Removal of volatile organic compounds from polluted air. J. Loss Prev. Process. Ind. https://doi.org/10.1016/S0950-4230(00)00007-3.
Khan, Z.U.H., Gul, N.S., Sabahat, S., Sun, J., Tahir, K., Shah, N.S., Muhammad, N., Rahim, A., Imran, M., Iqbal, J., Khan, T.M., Khasim, S., Farooq, U., Wu, J., 2023. Removal of organic pollutants through hydroxyl radical-based advanced oxidation processes. Ecotoxicol. Environ. Saf. 267, 115564 https://doi.org/10.1016/J.ECOENV.2023.115564.
Lee, M., Oh, J., 2011. Synergistic effect of hydrogen peroxide production and sonochemiluminescence under dual frequency ultrasound irradiation. Ultrason. Sonochem. https://doi.org/10.1016/j.ultsonch.2010.11.022.
Li, X., Liu, H., Zhang, Y., Mahlknecht, J., Wang, C., 2024. A review of metallurgical slags as catalysts in advanced oxidation processes for removal of refractory organic pollutants in wastewater. J. Environ. Manage. 352, 120051. https://doi.org/10.1016/j.jenvman.2024.120051.
Liu, H., Li, X., Zhang, X., Coulon, F., Wang, C., 2023. Harnessing the power of natural minerals: A comprehensive review of their application as heterogeneous catalysts in advanced oxidation processes for organic pollutant degradation. Chemosphere 139404. https://doi.org/10.1016/j.chemosphere.2023.139404.
Lu, X., Prosperetti, A., Toegel, R., Lohse, D., 2003. Harmonic enhancement of single-bubble sonoluminescence. Phys. Rev. E. 67, 56310 https://doi.org/10.1103/PhysRevE.67.056310.
Makino, K., Mossoba, M.M., Riesz, P., 1982. Chemical effects of ultrasound on aqueous solutions. Evidence for hydroxyl and hydrogen free radicals (.cntdot.OH and .cntdot.H) by spin trapping. J. Am. Chem. Soc. 104, 3537–3539. https://doi.org/10.1021/ja00376a064.
Makoś, P., Fernandes, A., Boczkaj, G., 2018. Method for the simultaneous determination of monoaromatic and polycyclic aromatic hydrocarbons in industrial effluents using dispersive liquid–liquid microextraction with gas chromatography–mass spectrometry. J. Separ. Sci. 41, 2360–2367. https://doi.org/10.1002/jssc.201701464.
Manickam, S., Zainal Abidin, N.B., Parthasarathy, S., Alzorqi, I., Ng, E.H., Tiong, T.J., Gomes, R.L., Ali, A., 2014. Role of H2O2 in the fluctuating patterns of COD (chemical oxygen demand) during the treatment of palm oil mill effluent (POME) using pilot scale triple frequency ultrasound cavitation reactor. Ultrason. Sonochem. https://doi.org/10.1016/j.ultsonch.2014.01.002.
Matafonova, G., Batoev, V., 2020. Dual-frequency ultrasound: strengths and shortcomings to water treatment and disinfection. Water Res. 182, 116016 https://doi.org/10.1016/j.watres.2020.116016.
Moholkar, V.S., 2009. Mechanistic optimization of a dual frequency sonochemical reactor. Chem. Eng. Sci. 64, 5255–5267. https://doi.org/10.1016/J.CES.2009.08.037.
Nan, H., Huang, R., Zhang, X., Wang, C., 2024. How does ball-milling elevate biochar as a value-added peroxydisulfate activator for antibiotics removal? Ind. Crop. Prod. 214, 118569. https://doi.org/10.1016/j.indcrop.2024.118569.
Nikolaou, S., Vakros, J., Diamadopoulos, E., Mantzavinos, D., 2020. Sonochemical degradation of propylparaben in the presence of agro-industrial biochar. J. Environ. Chem. Eng. 8, 104010 https://doi.org/10.1016/J.JECE.2020.104010.
Okouchi, S., Nojima, O., Arai, T., 1992. Cavitation-induced degradation of phenol by ultrasound. Water Sci. Technol. 26, 2053–2056. https://doi.org/10.2166/wst.1992.0659.
Pradhan, A.A., Gogate, P.R., 2010. Degradation of p-nitrophenol using acoustic cavitation and Fenton chemistry. J. Hazard Mater. 173, 517–522. https://doi.org/10.1016/j.jhazmat.2009.08.115.
Psillakis, E., Goula, G., Kalogerakis, N., Mantzavinos, D., 2004. Degradation of polycyclic aromatic hydrocarbons in aqueous solutions by ultrasonic irradiation. J. Hazard Mater. https://doi.org/10.1016/j.jhazmat.2004.01.004.
Rao, P.S., Hayon, E., 1975. Redox potentials of free radicals. IV. Superoxide and hydroperoxy radicals . O2- and ·HO2. J. Phys. Chem. 79, 397–402. https://doi.org/10.1021/j100571a021.
Rayaroth, M.P., Boczkaj, G., Aubry, O., Aravind, U.K., Aravindakumar, C.T., 2023. Advanced oxidation processes for degradation of water pollutants: ambivalent impact of carbonate species: a review. Water 15. https://doi.org/10.3390/w15081615.
Shen, Y., Xu, Q., Wei, R., Ma, J., Wang, Y., 2017. Mechanism and dynamic study of reactive red X-3B dye degradation by ultrasonic-assisted ozone oxidation process. Ultrason. Sonochem. https://doi.org/10.1016/j.ultsonch.2016.08.006.
Sivakumar, M., Pandit, A.B., 2001. Ultrasound enhanced degradation of Rhodamine B: optimization with power density. Ultrason. Sonochem. https://doi.org/10.1016/S1350-4177(01)00082-7.
Sivakumar, M., Tatake, P.A., Pandit, A.B., 2002. Kinetics of p-nitrophenol degradation: effect of reaction conditions and cavitational parameters for a multiple frequency system. Chem. Eng. J. https://doi.org/10.1016/S1385-8947(01)00179-6.
Sun, J.H., Sun, S.P., Sun, J.Y., Sun, R.X., Qiao, L.P., Guo, H.Q., Fan, M.H., 2007. Degradation of azo dye Acid black 1 using low concentration iron of Fenton process facilitated by ultrasonic irradiation. Ultrason. Sonochem. https://doi.org/10.1016/j.ultsonch.2006.12.010.
Sun, P., Liu, H., Feng, M., Zhang, X., Fang, Y., Zhai, Z., Sharma, V.K., 2021. Dual nonradical degradation of acetaminophen by peroxymonosulfate activation with highly reusable and efficient N/S co-doped ordered mesoporous carbon. Sep. Purif. Technol. 268, 118697 https://doi.org/10.1016/J.SEPPUR.2021.118697.
Swamy, K.M., Narayana, K.L., 2001. Intensification of leaching process by dual-frequency ultrasound. Ultrason. Sonochem. 8, 341–346. https://doi.org/10.1016/S1350-4177(01)00067-0.
Tatake, P.A., Pandit, A.B., 2002. Modelling and experimental investigation into cavity dynamics and cavitational yield: influence of dual frequency ultrasound sources. Chem. Eng. Sci. 57, 4987–4995. https://doi.org/10.1016/S0009-2509(02)00271-3.
Thanh Nguyen, T., Asakura, Y., Koda, S., Yasuda, K., 2017. Dependence of cavitation, chemical effect, and mechanical effect thresholds on ultrasonic frequency. Ultrason. Sonochem. 39, 301–306. https://doi.org/10.1016/J.ULTSONCH.2017.04.037.
Tian, W., Chen, S., Zhang, H., Wang, H., Wang, S., 2022. Sulfate radical-based advanced oxidation processes for water decontamination using biomass-derived carbon as catalysts. Curr. Opin. Chem. Eng. 37, 100838 https://doi.org/10.1016/J.COCHE.2022.100838.
Vellingiri, K., Choudhary, V., Kumar, S., Philip, L., 2022. Sorptive removal versus catalytic degradation of aqueous BTEX: a comprehensive review from the perspective of life-cycle assessment. Environ. Sci. Water Res. Technol. 8, 1359–1390. https://doi.org/10.1039/D1EW00918D.
von Gunten, U., 2003. Ozonation of drinking water: Part II. Disinfection and by-product formation in presence of bromide, iodide or chlorine. Water Res. 37, 1469–1487. https://doi.org/10.1016/S0043-1354(02)00458-X.
Wang, J., Wang, S., 2020. Reactive species in advanced oxidation processes: formation, identification and reaction mechanism. Chem. Eng. J. 401, 126158 https://doi.org/10.1016/j.cej.2020.126158.
Wang, Z., Fingas, M., Landriault, M., Sigouin, L., Xu, N., 1995. Identification of alkylbenzenes and direct determination of BTEX and BTEX + C3-benzenes in oils by GC/MS. Anal. Chem. 67, 3491–3500. https://doi.org/10.1021/ac00115a018.
Wang, S., Huang, B., Wang, Y., Liao, L., 2006. Comparison of enhancement of pentachlorophenol sonolysis at 20 kHz by dual-frequency sonication. Ultrason. Sonochem. 13, 506–510. https://doi.org/10.1016/J.ULTSONCH.2005.10.004.
Weavers, L.K., Ling, F.H., Hoffmann, M.R., 1998. Aromatic compound degradation in water using a combination of sonolysis and ozonolysis. Environ. Sci. Technol. 32, 2727–2733. https://doi.org/10.1021/es970675a.
Ye, L., Zhu, X., Liu, Y., 2019. Numerical study on dual-frequency ultrasonic enhancing cavitation effect based on bubble dynamic evolution. Ultrason. Sonochem. 59, 104744 https://doi.org/10.1016/J.ULTSONCH.2019.104744.
Yu, X.-Y., Barker, J.R., 2003. Hydrogen peroxide photolysis in acidic aqueous solutions containing chloride ions. I. Chemical mechanism. J. Phys. Chem. A 107, 1313–1324. https://doi.org/10.1021/jp0266648.
Yusof, N.S.M., Babgi, B., Alghamdi, Y., Aksu, M., Madhavan, J., Ashokkumar, M., 2016. Physical and chemical effects of acoustic cavitation in selected ultrasonic cleaning applications. Ultrason. Sonochem. 29, 568–576. https://doi.org/10.1016/j.ultsonch.2015.06.013.
Zanias, A., Frontistis, Z., Vakros, J., Arvaniti, O.S., Ribeiro, R.S., Silva, A.M.T., Faria, J.L., Gomes, H.T., Mantzavinos, D., 2020. Degradation of methylparaben by sonocatalysis using a Co–Fe magnetic carbon xerogel. Ultrason. Sonochem. 64, 105045 https://doi.org/10.1016/J.ULTSONCH.2020.105045.
Zhang, Y., Zhang, Y., Li, S., 2017. Combination and simultaneous resonances of gas bubbles oscillating in liquids under dual-frequency acoustic excitation. Ultrason. Sonochem. 35, 431–439. https://doi.org/10.1016/j.ultsonch.2016.10.022.

Zhao, L., Ma, J., Zhai, X., 2010. Enhanced mechanism of catalytic ozonation by ultrasound with orthogonal dual frequencies for the degradation of nitrobenzene in aqueous solution. Ultrason. Sonochem. 17, 84–91. https://doi.org/10.1016/J.ULTSONCH.2009.07.001.

Zhong, Z., Sha, Q., Zheng, J., Yuan, Z., Gao, Z., Ou, J., Zheng, Z., Li, C., Huang, Z., 2017. Sector-based VOCs emission factors and source profiles for the surface coating industry in the Pearl River Delta region of China. Sci. Total Environ. 583, 19–28. https://doi.org/10.1016/j.scitotenv.2016.12.172.

Zhou, T., Li, Y., Wong, F.S., Lu, X., 2008. Enhanced degradation of 2,4-dichlorophenol by ultrasound in a new Fenton like system (Fe/EDTA) at ambient circumstance. Ultrason. Sonochem. https://doi.org/10.1016/j.ultsonch.2008.01.005.